Evaluation of a mesoscale coupled ocean-atmosphere configuration for tropical cyclone forecasting in the South West Indian Ocean basin

Laetitia Corale[1]

[1]Doctorant

November 22, 2022

Abstract

The performance in term of tropical cyclone track and intensity prediction of the new coupled ocean-atmosphere system based on the operational atmospheric model AROME-Indian Ocean and the ocean model NEMO is assessed against that of the current operational configuration in the case of seven recent tropical cyclones. Five different configurations of the forecast system are evaluated: two with the coupled system, two with an ocean mixed layer parameterization and one with a constant sea surface temperature. For each ocean-atmosphere coupling option, one is initialized directly with the MERCATOR-Ocean PSY4 product as in the current operational configuration and the other with the ocean state that is cycled in the AROME-NEMO coupled suite since a few days before the cyclone intensification. The results show that the coupling with NEMO improves the intensity of cyclones in AROME-IO, especially when they encounter a slow propagation phase. For short-term forecasts (less than 36 hours), the presence of a cooling in the initial state that has been triggered by the AROME high-resolution cyclonic winds in a previous coupled forecast already improves the tropical cyclone intensity for all coupled or uncoupled configurations. However, the simplification of the ocean-atmosphere interactions in the configurations using the ocean mixed layer parameterization is not the only reason for the overestimation of the intensity of already well-developed TC in AROME-IO. The impact of other model components, such as the air-sea flux parameterization and the cloud microphysics scheme will need to be further investigated.

Evaluation of a mesoscale coupled ocean-atmosphere configuration for tropical cyclone forecasting in the South West Indian Ocean basin

Laëtitia Corale[1], Sylvie Malardel[1], Soline Bielli[1], Marie-Noëlle Bouin[2,3]

[1]Laboratoire de l'Atmosphère et des Cyclones (LACy), Université de La Réunion, CNRS, Météo-France, 97400 Saint-Denis, France

[2]CNRM, Université de Toulouse, Météo-France, CNRS, 31057 Toulouse, France

[3]Laboratoire d'Océanographie Physique et Spatiale, Université de Brest, CNRS, Ifremer, IRD, IUEM, 29280 Plouzané, France

Key Points:

- The numerical weather prediction coupled ocean-atmosphere model AROME-IO/NEMO improves the regional forecast of Tropical cyclone in the South West Indian Ocean when compared to the current operational configuration for which the ocean is reduced to a simple 1D ocean mixed layer parameterization.
- The improvement mostly comes from quasi-stationary or very slow moving intense cyclones.
- In an operational suite, the fast and small scale features which are triggered in the ocean by the high resolution cyclonic winds from the mesoscale atmospheric model must be cycled from one coupled forecast to the next one in order to keep a memory of the ocean-atmosphere interactions in the vicinity of the TC.

Corresponding author: Sylvie Malardel, `sylvie.malardel@meteo.fr`

Abstract

The performance in term of tropical cyclone track and intensity prediction of the new coupled ocean-atmosphere system based on the operational atmospheric model AROME-Indian Ocean and the ocean model NEMO is assessed against that of the current operational configuration in the case of seven recent tropical cyclones. Five different configurations of the forecast system are evaluated: two with the coupled system, two with an ocean mixed layer parameterization and one with a constant sea surface temperature. For each ocean-atmosphere coupling option, one is initialized directly with the MERCATOR-Ocean PSY4 product as in the current operational configuration and the other with the ocean state that is cycled in the AROME-NEMO coupled suite since a few days before the cyclone intensification. The results show that the coupling with NEMO improves the intensity of cyclones in AROME-IO, especially when they encounter a slow propagation phase. For short-term forecasts (less than 36 hours), the presence of a cooling in the initial state that has been triggered by the AROME high-resolution cyclonic winds in a previous coupled forecast already improves the tropical cyclone intensity for all coupled or uncoupled configurations. However, the simplification of the ocean-atmosphere interactions in the configurations using the ocean mixed layer parameterization is not the only reason for the overestimation of the intensity of already well-developed TC in AROME-IO. The impact of other model components, such as the air-sea flux parameterization and the cloud microphysics scheme will need to be further investigated.

Plain Language Summary

The ocean provides the energy for the intensification and persistence of tropical cyclones through warm sea surface temperature and sea-air heat and moisture exchanges. But, the ocean-atmosphere interactions also trigger processes which cools the sea surface temperature beneath the tropical cyclone and thus generates a negative feedback on the TC intensification.

The numerical forecasts of the regional numerical weather prediction model AROME-IO are valuable guidance for the Regional Specialized Meteorological Centre for Tropical Cyclones of La Réunion. Currently, AROME-IO interacts with a very simplified model of the first well mixed layer of the ocean. The ocean mixed layer model is able to reproduce the turbulent mixing near the ocean surface, but its reduced physics does not allow the larger scale horizontal and vertical transport by the currents. A coupling between the atmospheric model and a full ocean model is necessary to take into account the advective transport responsible for the upwellings and thus represent all the processes contributing to the cooling of the ocean during the passage of a TC. The objective of our study is to evaluate the possibility of replacing the current ocean mixed layer parameterization by the ocean model NEMO in the operational configuration of AROME-IO. Overall, we found that the new coupling improves the cyclone intensity in AROME-IO both in terms of bias and standard deviation. These improvements come almost entirely from tropical cyclones that encounter a slow propagation phase (less than 2 m s^{-1} for at least 12 hours). For short-term forecasts (less than 36 hours), the presence of a cooling that is triggered by AROME high-resolution cyclonic winds in the initial state of the ocean already improves the TC intensity forecast, even when the ocean mixed layer parameterization is used.

1 Introduction

Tropical cyclones (TCs) can be associated with a devastating combination of several hazardous phenomena: storm surges, floods, extreme winds, tornadoes and lightnings. They are highly destructive atmospheric phenomena that cause damage to life and infrastructures along tropical coastal areas, particularly in the South West Indian Ocean (SWIO: 30-90° E, 0-40° S) tropical islands, where economic vulnerability, fragile infrastructures and confined space make populations highly vulnerable to cyclonic hazards. The SWIO accounts for an average of 12% of annual global cyclone activity with about ten tropical storms, four of which reach the stage of a tropical cyclone (equivalent CAT2-3 on the US Saffir-Simpson scale, see Leroux et al., 2018). Forecasters of the Regional Specialised Meteorological Centre for Tropical Cyclones (RSMC-Cyclones) of La Réunion are in demand of accurate forecasts of the track and intensity of TC to quickly identify potentially impacted areas and effectively warn communities of the impending danger.

The work carried out in recent years has particularly led to improvements in the forecasting of TC tracks (Courtney et al., 2019; Heming et al., 2019). TC intensity is less predictable as it involves small scales features which are not yet well understood. The implementation of coupled ocean-atmosphere (OA) numerical weather prediction (NWP) systems has however been recognised as one of the key elements of the progress for TC intensity forecasting (Yablonsky, 2016; Mogensen et al., 2017; Feng et al., 2019; Vellinga et al., 2020). Accurate modelling of OA interactions is particularly crucial in the SWIO basin, where atmospheric variability is associated with a particularly strong oceanic response (and vice versa). It is considered as the cyclonic basin with the highest prevalence of OA interactions (Vialard et al., 2008) due to the unique thermocline structure in the Seychelles-Chagos thermocline ridge area (55-70°E, 5-15°S) (Hermes & Reason, 2009).

The ocean provides the energy for the intensification and persistence of TCs through warm sea surface temperature (SST) and air-sea heat and moisture fluxes. But, the OA interactions also trigger processes which cools the SST beneath the TC and thus generates a negative feedback on the TC intensification (Srinivas et al., 2016).

The sea surface cooling is governed by three different processes: 1) loss of energy associated to the heat and evaporation fluxes towards the atmosphere, 2) turbulent vertical mixing in the upper ocean which incorporates colder water at the bottom of the ocean mixed layer (OML), and 3) upwelling of deeper cold water generated by Ekman pumping (Price, 1981; Black, 1983; Bender et al., 1993). The respective part of these different processes depend largely on the cyclone intensity and ocean preconditioning (Vincent et al., 2012b). According to Vincent et al. (2012b) and Jullien et al. (2012), the surface heat fluxes are dominant for weak to medium intensity cyclones, while the turbulent mixing accounts for 30 to 50% of the surface cooling for weaker cyclones but for more than 80% for the most intense. The effect of the upwelling of colder water increases with the cyclone intensity to reach 20% for the most intense cyclones. Especially, its effect is crucial to explain the asymmetry of the cold wake with respect to the cyclone direction. By not coupling the atmosphere with the ocean, the ocean acts as an infinite energy source for the TCs. Coupled OA models introduce a negative feedback between the TC and the SST. Although the effect of the surface heat fluxes and turbulent mixing can be represented by a one-dimensional (1D) parameterization of the OML, the effect of the upwellings can only be represented by a three-dimensional (3D) ocean model (Yablonsky & Ginis, 2009; Mogensen et al., 2017). Numerous studies have thus shown the benefit of accounting for the upwelling effect in a 3D ocean model for TC forecasting (Ginis, 2002; Bender et al., 2007; Yablonsky & Ginis, 2009; Jullien et al., 2014; Mogensen et al., 2017; Bielli et al., 2021).

The strength of the negative feedback between the TC and the ocean and the cooling of the surface waters is influenced by different factors; the slow translation speed and shallow depth of the OML appear to favour greater SST cooling and negative feedback (Schade & Emanuel, 1999). Using a simple coupled model, Schade and Emanuel (1999) suggest a range of 10-60% decrease in storm intensity as a function of storm speed. Similarly, Yablonsky and Ginis (2009) demonstrate the importance of a 3D ocean model for resolving SST cooling when simulating a TC moving at a speed of 5 m s^{-1} and even more critical for slower systems. Other subsurface ocean features such as the thermocline stratification due to salt layers for instance or fine scales structures associated with fronts and eddies also have the potential to affect storm intensity (Schade & Emanuel, 1999; Bao et al., 2000; Lin et al., 2008; Vincent et al., 2012a; Jullien et al., 2014). For example, the deeper mixed layer of warm-core eddies is known to favour TC intensification (Chang & Anthes, 1978; Bao et al., 2000).

The mesoscale numerical weather prediction model "Applications de la Recherche à l'Opérationnel à Méso-Echelle - Indian Ocean " (AROME-IO) provides 4 times a day a forecast for a large SWIO domain. During the SWIO TC season, AROME-IO products provide valuable information on TC intensity to the RSMC-Cyclones of La Réunion. In its current operational version, AROME-IO is coupled every 5 minutes to a 1D parameterization of the OML that takes into account the rapid change of the SST due to the OA heat exchanges and the turbulent mixing of the OML that is triggered by cyclonic winds.

The objective of this study is to analyse the impact of replacing the current 1D OML parameterization by a fully 3D coupling with the ocean model NEMO (The Nucleus for European Model of the Ocean, Madec et al., 2019) in the operational high resolution mesoscale cloud model AROME-IO (Seity et al., 2011; Bousquet et al., 2020) used by the RSMC of La Réunion. This paper does not aim at analysing in detail the OA processes in TC case studies as the current knowledge of the main OA interaction mechanisms in a TC is already quite advanced and well documented. It rather focuses on the impact of changing the representation of the ocean component in the forecast system in term of TC forecast. Thus, five configurations of the AROME-IO modelling system has been set up for this study. Numerical simulations have been performed for a selection of seven TCs that developed over the SWIO basin during the 2018-2019 and 2019-2020 cyclone seasons, and the TC Batsirai, which occurred during the 2021-2022 cyclone season. This large set of forecasts has then been analysed in order to assess the impact of the coupling in terms of track, intensity and structure of the TCs.

The plan of the paper is as follows. Section 2 presents the forecast system AROME-IO, the experimental coupled system AROME-IO/NEMO and the description of the different numerical simulations performed in this study. The results of these simulations are analysed in section 3. First, the statistical impact of the 3D OA coupling and the choice of initial conditions is assessed with scores against the Best-Track (BT) data for a large number of TC simulations. Second, the main conclusions of scores analysis are illustrated with three TC cases, Gelena (quasi-stationary) and Belna (regular propagation velocity of about 5 m s^{-1}), and Batsirai, for which buoy measurements enable a direct comparison of the modelled cooling effects with observations. Conclusions and perspectives are given in section 4.

2 Tools, methods and data

In this section, we give a short description of the numerical systems used for this study. We then describe the 5 different types of simulations which have been performed for 31 initial dates and which are analysed in section 3.

2.1 The AROME-IO operational system

AROME-IO (see Faure et al. (2020) and Bousquet et al. (2020) for more details) is an overseas version of the AROME-France model, which is the operational convection permitting, limited area, numerical weather prediction model used at Météo-France since 2008. Since 2016, AROME-IO produces 48 hours forecasts (78 h on demand) 4 times a day over an area of 3000 km by 1400 km (30°E-70°E, 7°S-22°S) encompassing most islands of the SWIO. Its horizontal resolution is 2.5 km and the time step is 60 s. In the vertical, 90 levels are distributed between the surface (first level at 5 m and 34 levels within the first 2 km) and 10 hPa. The AROME-IO operational configuration is initialised from the High RESolution Integrated Forecasting System (HRES IFS) European Centre for Medium-Range Weather Forecasts (ECMWF) model (currently about 9km horizontal resolution), which also provides the lateral boundary conditions at the frequency of 1h. An IAU (Incremental Analysis Update; Bloom et al., 1996) initialisation scheme is used to built the small-scale features and to reduce the model spin-up at initial time t_0. The IAU algorithm combines the ECMWF larger scale analysis increments (temperature, wind, humidity, and surface pressure) valid at t_0 with a 6 hour AROME-IO forecast initialised directly from the ECMWF analysis at $(t_0 - 6)$ hours.

The atmosphere-sea surface exchanges are represented by the Exchange Coefficient Unified Multi-campaign Experiments (ECUME) parameterization (Weill et al., 2003; Belamari, 2005) which is part of the EXternalised SURface platform SURFEX (Voldoire et al., 2017). Moreover, AROME-IO is coupled every 300 s to a 1D OML model (Gaspar et al., 1990; Lebeaupin Brossier et al., 2009) in order to better take into account the feedback between the atmosphere and the ocean in cyclonic conditions. In the current configuration, the OML prognostic parameters (salinity, temperature and currents) are initialised from the first 26 levels (depth of about 180 m) of the MERCATOR-Ocean global product PSY4 (Lellouche et al., 2018) which are available every 6 hours (1h means).

The 1D OML parameterization is built on a partial representation of the ocean processes which are triggered by winds. The advection and pressure gradient terms are neglected in the system of dynamic and thermodynamic equations. The water columns are therefore independent of each others. As a consequence, there is no vertical velocity generated by the divergence or convergence of currents and thus no upwelling and downwelling. The OML model reproduces only the turbulent exchanges between the ocean and the atmosphere and the turbulent mixing thanks to a 1.5 order turbulent scheme directly adapted for the ocean from the Turbulent Kinetic Energy (TKE) scheme used in AROME (Bougeault & Lacarrere, 1989).

In a limited area model, the TCs track are mostly driven by the large scale environment of the TCs. In AROME, they usually follow the IFS scenario. The score of the short term AROME forecast in term of TC position error is then very similar to the one of the HRES IFS (Fig 1 (a)). The mesoscale model AROME significantly improves the short term forecast of TC intensification compared to the HRES-IFS model which regularly underestimates TC intensities (Fig 1 (b-c)). AROME shows however a general tendency to overestimate the TC intensification of the most intense systems. One of the expectation of the better representation of the interaction between the cyclonic circulation and the oceanic surface in the OA coupled model is actually a reduction of the TC intensity due to the generation of a cold upwelling underneath. We will see in the following sections that it actually contributes to the reduction of the positive bias error in intensity, even if other factors may also explain AROME overactivity.

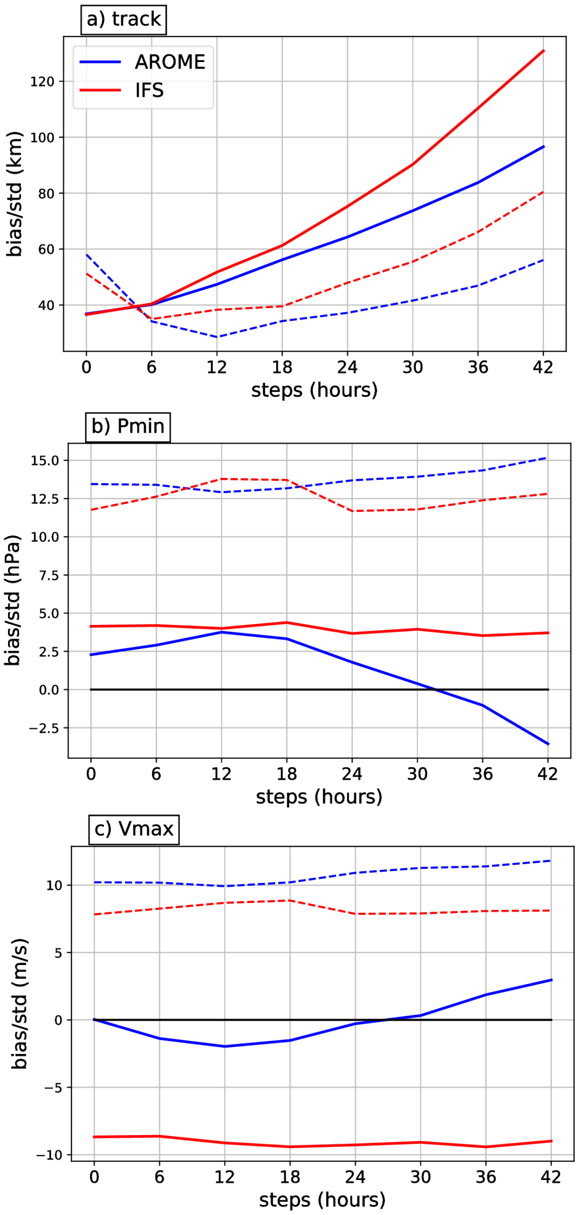

Figure 1.

Bias (solid lines) and standard deviation (dashed lines) for (a) the TC centre position, (b) the minimum of pressure at the centre of the TC and (c) maximal 10-m wind in the TC wall for IFS (red) and AROME-IO (blue) against the BT for all TCs of the 2018-2019 and 2019-2020 in the AROME-IO domain.

2.2 The AROME-NEMO coupled system

The experimental coupled system AROME-NEMO which has been implemented in the context of this work combines the AROME-IO atmospheric model (Faure et al.,

2020) and a regional version of the NEMO ocean model (Madec et al., 2019). The coupling between these two components is controlled by the OASIS3-MCT coupler (Craig et al., 2017).

NEMO is the European modelling framework for oceanographic research, operational oceanography, seasonal forecasting and climate studies. This study uses the version 3.6 of the code with the same ORCA grid (tripolar grid with variable horizontal resolution; Madec & Imbard, 1996) at the horizontal resolution of a 1/12° (about 9 km in the SWIO region) and the same 50 unevenly spaced vertical levels as the PSY4 global operational products of MERCATOR-Ocean. The NEMO domain covers the whole oceanic part of AROME-IO. The bathymetry is based on the ETOPO1 database (Amante & Eakins, 2009). The vertical mixing is a TKE closure scheme based on the work of Gaspar et al. (1990) (like the 1D OML used in this study), but with important modifications introduced by Madec et al. (1998) in the implementation and formulation of the mixing length scale.

NEMO provides to OASIS the 1h mean SST at a coupling frequency of 1 h. The SST is used to compute the air-sea fluxes at each subsequent atmospheric time step. The effect of surface currents on surface fluxes and atmospheric low-level flow is not considered in this study. Previous studies have shown little impact of currents on air-sea fluxes, especially in comparison to the uncertainty associated with OA interactions in strong winds (Pianezze et al., 2018; Bouin & Lebeaupin Brossier, 2020). The 1 h mean solar and net heat fluxes and the components of the horizontal wind stress and atmospheric freshwater are returned to OASIS by SURFEX and then sent to NEMO with a 1h coupling frequency (Figure 2). The corresponding equations and the description of the coupling strategy are detailed in Voldoire et al. (2017).

On the Météo-France supercomputers, the extra computing cost of the oceanic model at a 1/12° resolution and a coupling frequency of 1 hour is negligible compared to the cost of the atmospheric model. For example, the current prototype runs on 480 processors for AROME-IO against only 32 processors for NEMO. So, the computing cost would not be a limitation for a potential operational use of the coupled system. However, if this configuration was meant to become operational with 4 runs a day, an important technical work would be needed in order to automate the processing of the NEMO initial and lateral boundary condition files in real time. In the absence of a coupled data assimilation system for AROME-IO, the design of the ocean initial condition in an operational suite with the coupled system is an open scientific question that we have started to address in the present work. But, the question of ”coupled” initial conditions for the downscaling of both an atmospheric (IFS) and oceanic (MERCATOR-Ocean) state is a complex subject in itself that will need to be further investigated prior to an operational implementation.

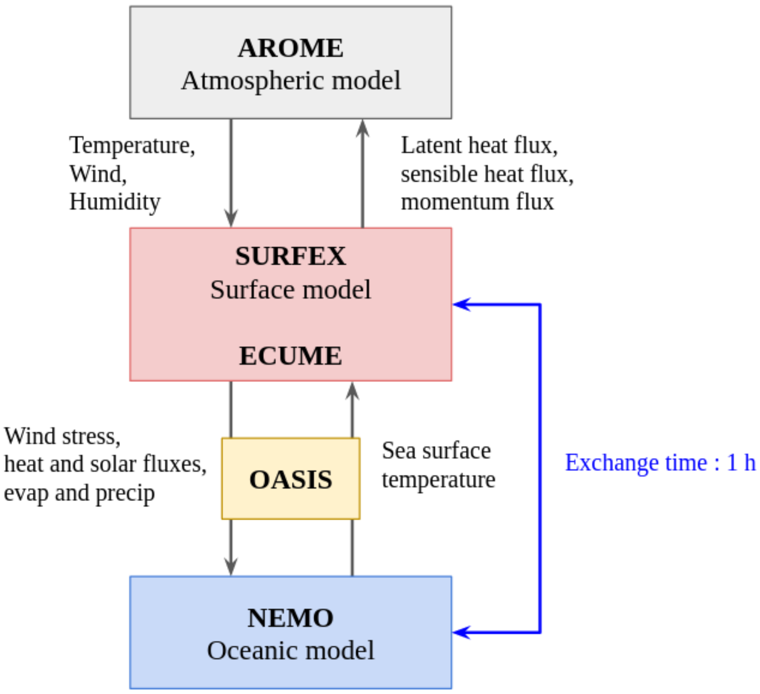

Figure 2. Schematic diagram of the coupling between AROME and NEMO via SURFEX and OASIS.

2.3 Description of the TC simulations

The main objective of this study is to evaluate the sensitivity of the AROME-IO TC forecasts skill to the representation of the ocean underneath.

Five different configurations have been implemented (Table 1). In the first configuration, the SST field is initialised with the PSY4 ocean state and it is kept constant in the forecast. This configuration has been used in AROME-IO between 2016 and the end of 2017, prior to the implementation of the OML parameterization. It is also still the configuration of AROME-France.

Table 1. Summary of the 5 simulation types which are analysed in this work

	SST cst	OMLpsy4	OMLcyO	CPLpsy4	CPLcyO
Ocean configuration	None	1D OML	1D OML	3D ocean	3D ocean
Initial ocean state	PSY4	PSY4	Cycled Ocean	PSY4	Cycled Ocean

Then, the OML parameterization is switched on for two configurations and the new coupled system AROME-IO/NEMO is used for the last two configurations.

As an other objective of this work is to advice on the design of a future coupled operational system, two different solutions for the initial oceanic state have been used for both the OML and the coupled simulations. In a first solution, the ocean model directly initialised with the PSY4 products provided by MERCATOR-Ocean. Such a solution is currently used in operation to initialise the OML at the beginning of each new forecast. In our study, we used this solution both for the OML configuration (later referred to as OMLpsy4, which corresponds to the configuration of the current operational system) and the coupled AROME-NEMO configuration (referred to as CPLpsy4).

As the state of the ocean in the PSY4 global products is quite "smooth", the SST cooling and the upwelling generated by TCs is much weaker than in the AROME-NEMO coupled configuration (see discussion in section 3). Test simulations (not shown) with a forced configuration of NEMO using IFS or AROME winds showed that the main reason explaining the difference of SST cooling induced by TC circulations between PSY4 and AROME-NEMO is the strength of the winds forcing the ocean. As pointed out by several recent studies, strong winds in the ECMWF IFS- WAve Model (WAM) configuration are generally underestimated (Pineau-Guillou et al., 2018; Haiden et al., 2018; Magnusson et al., 2019) whereas the wind from the current AROME-IO operational system are much closer to the wind estimated by the BT (Bousquet et al., 2020; see also Fig 1). We then decided to set up a second solution in which the ocean model is initialized by an ocean state resulting from a previous AROME-NEMO coupled run. In practice, the coupled simulations start about a week before the TC enters the AROME domain. The first coupled simulation is initialised with PSY4, then, 24 h later, the next

NEMO simulation starts from the state of the ocean of the 24 h forecast of the previous coupled simulation (configuration referred to as CPLcyO). The "cycled" state of the ocean is also used to initialised the OML of an other series of simulations referred to as OMLcyO. Cycling the ocean without any relaxation toward observation is a solution which can be used only for a few days in a row. But, in the context of the TCs simulations conducted for this study, we think that this second solution emulates a forecast suite where the ocean would be initialised by an ocean analysis forced with the AROME winds instead of the IFS winds or by a combination between a smooth ocean analysis and an oceanic state issued from a previous coupled AROME-NEMO run.

In order to focus on the sensitivity to the ocean initial conditions, all five configurations start from the same atmospheric state which is taken from the operational AROME-IO model. This means that the 6 h warmup is done with the OMLpsy4 configuration and the result is used as the initial condition of all five configurations. A few tests have been done with the same configuration both in the warmup and the 72h forecast. But, the spread in the TC characteristics after the warmup made the comparison between the different oceanic configuration difficult, hence our choice to start all configurations with the same atmospheric state for this study.

For each configuration, we have then set up a "light" NWP suite with only one 72 h forecast per day, at 00 UTC. The CPLcyO and OMLcyO suites start a few day before a TC enters the AROME-IO domain. The five suites have been run for seven different TCs that have been selected for various tracks and intensities (see Table 2) and with reasonable track prediction. The tracks of the seven cyclones are shown in Figure 3 and their intensity is indicated by colour dots corresponding to the five categories used in the SWIO basin: Tropical Depression (TD, $13 < \text{Vmax} < 16$ m s^{-1}), Moderate Tropical Storm (MTS, $17 < \text{Vmax} < 24$ m s^{-1}), Strong Tropical Storm (STS, $25 < \text{Vmax} < 32$ m s^{-1}), Tropical Cyclone (TC, $33 < \text{Vmax} < 43$ m s^{-1}), and Intense Tropical Cyclone (ITC, Vmax > 44 m s^{-1}) where Vmax is the 10 min averaged maximum wind speed.

For each suite, 31 forecasts have been produced; grouping seven TCs, with one to six starting times each, corresponding to the 31 initial times given in Table 3. As in the current operational system, large initial intensity errors are sometimes inherited from the IFS analysis despite the 6 h warmup. In such cases, we focuses on the differences between the five configurations rather than on a comparison with the BT.

Table 2. Name and characteristics of the selected TCs.

	SWIO classification	Maximum average wind (m s^{-1})	US Saffir-Simpson scale
Gelena	Intense tropical cyclone	57	CAT3
Idai	Intense tropical cyclone	49	CAT2
Kenneth	Intense tropical cyclone	57	CAT3
Belna	Tropical cyclone	42	CAT1
Calvinia	Tropical cyclone	33	CAT1
Diane	Moderate tropical storm	21	Tropical storm
Herold	Intense tropical cyclone	46	CAT2
Batsirai	Intense tropical cyclone	57	CAT3

Table 3. List of the 31 forecasts used for the statistics. Dates in bold include a period when the TC is quasi-stationary (slow moving): translation speed ≤ 2 m s^{-1} for at least 12 h.

Gelena	Idai	Kenneth	Belna	Calvinia	Diane	Herold
05/02/2019	**09/03/2019**	23/04/2019	06/12/2019	26/12/2019	23/01/2020	13/03/2020
06/02/2019	**10/03/2019**		07/12/2019	27/12/2019	24/01/2020	**14/03/2020**
07/02/2019	**11/03/2019**		08/12/2019	28/12/2019	25/01/2020	**15/03/2020**
08/02/2019	12/03/2019		09/12/19	29/12/2019		**16/03/2020**
09/02/2019	13/03/2019			**30/12/2019**		17/03/2020
10/02/2019	14/03/2019					18/03/2020

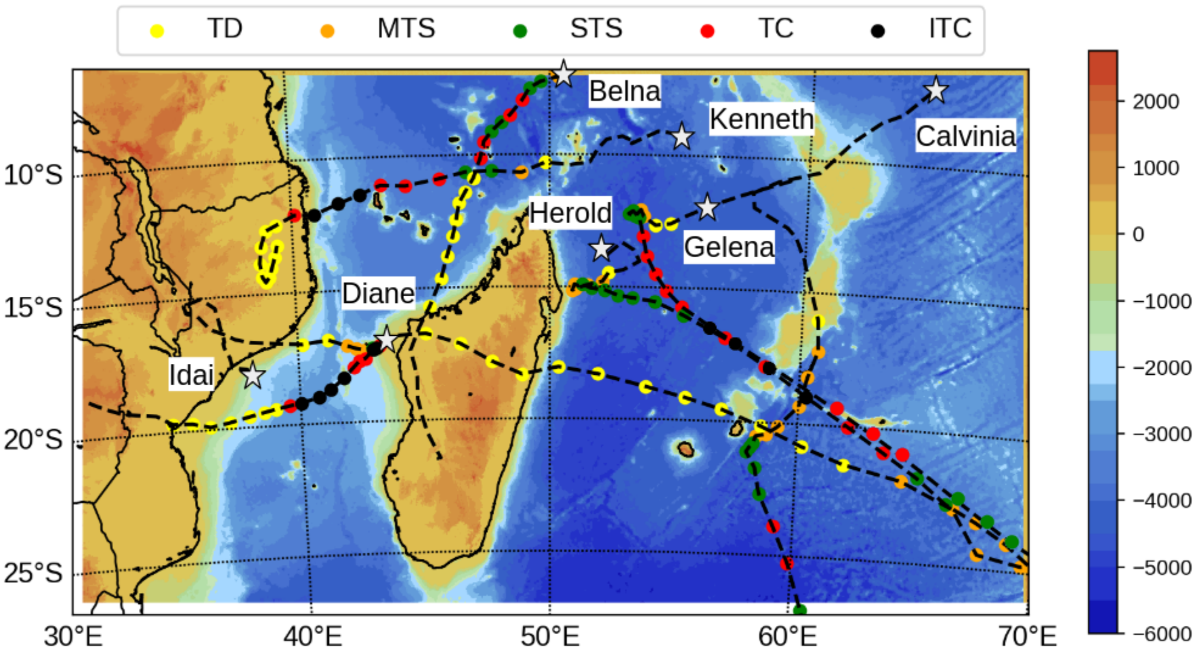

Figure 3. Orography and bathymetry (shading, in m) of the AROME-IO/NEMO coupled system. Track and intensity of Gelena, Idai, Kenneth, Belna, Calvinia, Diane and Herold as estimated by the RSMC of La Reunion. See text for the definition of the SWIO intensity classification.

3 Results

The aim of this section is to evaluate the coupled OA configuration and estimate its viability in an operational forecasting context. The first part of the section is a statistical analysis of the 31 runs which have been produced for each of the 5 model configurations. The second part of the section focuses on two particular cyclone cases which have been chosen according to their translation speed, the oceanic conditions at the beginning of the simulation and their impact on the ocean.

Compared to the Atlantic or North Pacific basin, the SWIO basin is very poor in both atmospheric and oceanic observational data. We then mainly use the BT data for the evaluation of the track and intensity of the TC. When available, we will also add comparison to the the SAR (Synthetic Aperture Radar) observations for the evaluation of stronger surface winds (available at https://cyclobs.ifremer.fr/app/; Mouche et al., 2017). Ocean sensors such as ARGO profilers or moored buoys (available at http://www.coriolis.eu.org/Data-Products/Data-selection) are rare and often far from the cyclonic area of interest. SST measurements from Earth observation satellites are usually very incomplete because of the heavy cloud cover in TC condition. It is therefore quite difficult to provide an accurate validation of the temperature predictions of ocean models in cyclonic conditions. A comparison between the modelled oceanic state and observation from a drifting buoy has been exceptionally possible in the case of TC Batsirai. It is shown in section 3.4.

3.1 Scores against the Best-Track

The TCs are tracked in all 31 forecasts of each of the 5 configurations (Table 3 and Table 1).

The TCs minimum mean sea level pressure (Pmin) and Vmax are then compared to the data of the objective analysis of the RSMC-La Réunion which is considered as the reference in this study (it is later referred to as BT). The Pmin bias and standard deviation against the BT are shown in Figure 4. Conclusions are very similar for Vmax (not shown).

Both constant SST runs (green curves) and OML runs (blue curves) overestimate the intensity of the TCs with a bias of more than 10 hPa after 72 hours of simulation. The OML simulations show however a slightly reduced bias between +48 and +60 hours of simulation and a better standard deviation than the constant SST runs. As expected, the systematic bias is significantly reduced by the 3D coupling with NEMO (pink curves). The standard deviation after 30 hours of simulation is also improved in the 3D coupled forecasts. The TCs characteristics in the OMLcyO simulations remains close to the ones in the CPLcyO runs for about 24 hours but then, the scores of the OMLcyO runs quickly degrade and reach the same bias and standard deviation as the runs with the operational configuration OMLpsy4.

As we expect the slow or quasi-stationary TCs to be the most sensitive to the 3D coupling with NEMO, we have split the original 31 dates into 2 groups. A first group, later referred to as slow TCs, contains runs for which the translation speed of the TC is less than or equal to 2 m s^{-1} for at least 12 hours (10 runs in Table 3). The remaining runs (21 runs) form a second group of regular or fast moving TCs. For simplicity, we will later referred to group 2 as ”fast” TCs . The statistics have been recomputed for each group (Figure 5).

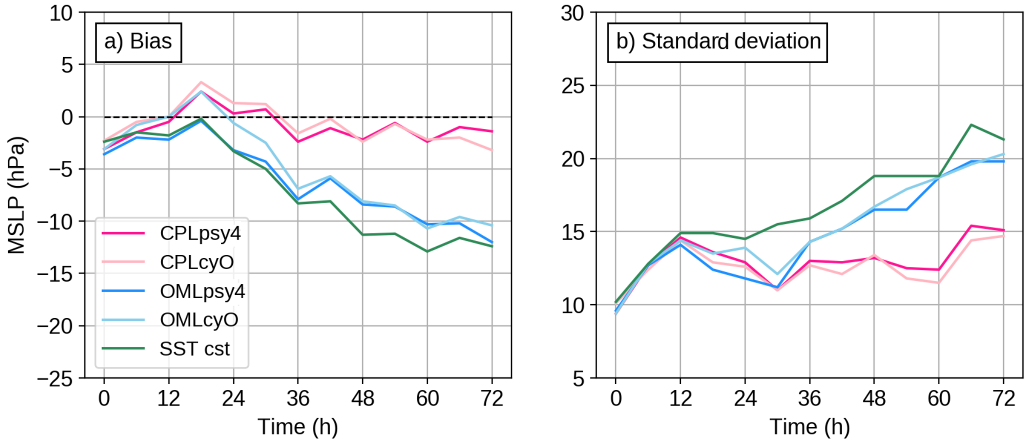

Figure 4. a) Bias and b) standard deviation for Pmin (hPa) derived from CPLpsy4 (dark pink), CPLcyO (light pink), OMLpsy4 (dark blue), OMLcyO (light blue) and SST constant (green) simulations against the BT. The statistics are based on 31 runs (corresponding to the different initial times) for 7 different TCs.

Figure 5 shows the Pmin bias (left) and standard deviation (right) against the BT data for the slow (top) and fast (bottom) groups. It clearly confirms that the 3D coupling between AROME and NEMO really matters for the intensity of the slow-moving storms with the bias of the OML simulations 20 hPa larger after 72 hours than the one in the CPL simulations. The impact of the 3D coupling is much smaller for the fast-moving TCs, with a tendency for the coupled runs, but also the OML run starting from the cycled ocean state to weakly underestimate the intensity of the TCs in the first 24 h. The behaviour of the model at the beginning of these simulations may be improved in a configuration where the 6 h IAU warmup uses the same configuration as the forecast. It is not the case here as all runs starts with the same initial atmospheric condition that is the result of the IAU warmup of the operational configuration (OMLpsy4). The coupled runs and OMLcyO may suffer from a spin-up period as the atmospheric boundary layer and the ocean adjust to each other and thus delay the intensification. More work would be needed to improved the consistency between the atmospheric and oceanic initial conditions in order to palliate the lack of OA coupled data assimilation, but this is beyond the scope of the present study.

In summary, the scores against the BT suggest that :

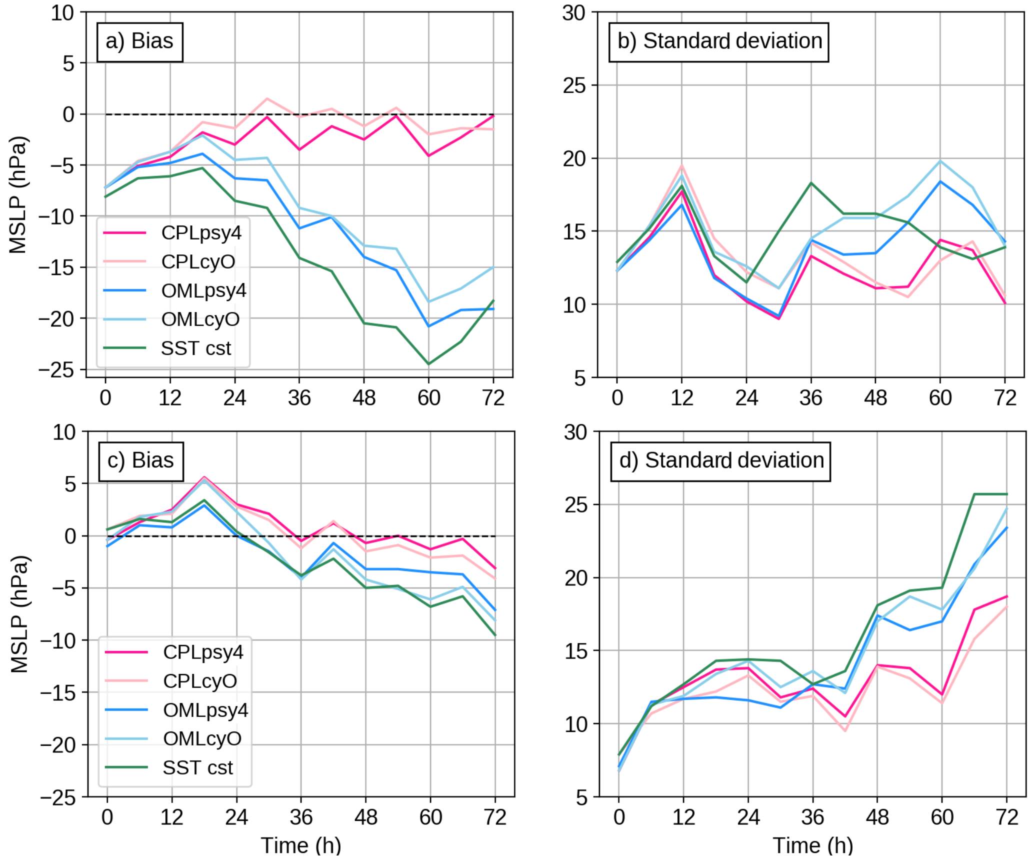

Figure 5. (a-c) bias and (b-d) standard deviation for Pmin (hPa) derived from CPLpsy4 (dark pink), CPLcyO (light pink), OMLpsy4 (dark blue), OMLcyO (light blue) and SST constant (green) simulations against the BT for (a-b) slow-moving storms (TC velocity ≤ 2 m s^{-1} for a minimum of 12 h) and (c-d) fast-moving storms.

- The 3D coupling statistically improves the estimation of the TC intensification in AROME-IO after 24/30 h of simulation,
- but the OA feedback allowed by the 3D coupling only significantly impact the intensity of slow storms.
- The cooling in the oceanic initial conditions that is consistent with the AROME wind forcing only impacts the first 24 hours of the TC intensity forecast when the OML parameterization is later used in the forecast model (OMLcyO).

In the following section, we analyse with more details the oceanic and the atmospheric responses in the new OA coupled system for three particular cases: TC Gelena from the "slow" group, TC Belna from the "fast" group and TC Batsirai for which we have drifter observations.

3.2 Gelena: a case of extreme cooling of the ocean in AROME-NEMO

3.2.1 Gelena analysis by the RMSC-La Réunion

Gelena was the ninth tropical storm of the 2018-2019 cyclone season in the SWIO. Gelena formed within an active monsoon trough taking place in early February 2019 over the SWIO from an area of low pressure located less than 1000 km east of Diego-Suarez (northern tip of Madagascar). It encountered a rapid development late on 5 February 2019 and the system became a TS in the early hours of 6 February. It reached the level of STS, almost TC (equivalent CAT2 on the US Saffir-Simpson scale) at the end of 6 February. It weakened on 7 February due to the cooling of the SST induced by its very slow motion on 6 and 7 February. Gelena accelerated after 7 February and resumed its intensification. It became a TC on the morning of 8 February, then it reached the stage of ITC (equivalent CAT3) 24 hours later. Gelena reached its maximum intensity in the early afternoon of 9 February with maximum winds estimated over 10 minutes at 57 m s^{-1} (equivalent CAT4) and a minimum sea level pressure of 938 hPa before weakening due to vertical shear. At the end of the night of 9 February, Gelena approached within 60 km of Rodrigues Island as ITC. The island suffered violent wind gusts recorded at 46 m s^{-1} at Pointe-Canon. During the following days, Gelena moved along a south-east and then east-south-east track and slowly filled in and dissipated at the end of 16 February east of 90°E in the subtropics.

Both the operational models IFS and AROME-IO overestimated the intensity of TC Gelena compared to that estimated by the BT. We suspected that the quasi-stationary behaviour of Gelena on 6 February and most part of 7 February led to a strong oceanic response which could have been underestimated by the IFS and the current OMLpsy4 configuration of AROME-IO. We will see in the next section that AROME-NEMO actually triggers a very intense upwelling on 6 February. After 24 h of simulation, the state of the ocean in the 6 February run is much cooler than the corresponding PSY4 analysis. The run of 7 February 2019 is then a good case to analyse the impact of the oceanic initial condition as the cyO and psy4 simulations do start with significantly different ocean conditions.

3.2.2 Simulations of TC Gelena

In this section, the development of TC Gelena and the corresponding response of the ocean are analysed with 2 sets of 5 runs starting 6 February 2019, 00 UTC and 7 February 2019, 00 UTC.

The TC tracks (Figure 6a) simulated with the CPL (pink curves), OML (blue curves) and SST constant (green line) configurations are similar and close to the BT that is estimated by the RSMC-La Réunion (black line), despite a slight shift to the west after the 8 February 2019, 06 UTC. The mean error (including both along track and across track errors) is approximately 30 km during the first 30 h of the simulations and it reaches about 200 km at the end of the 72h simulations .

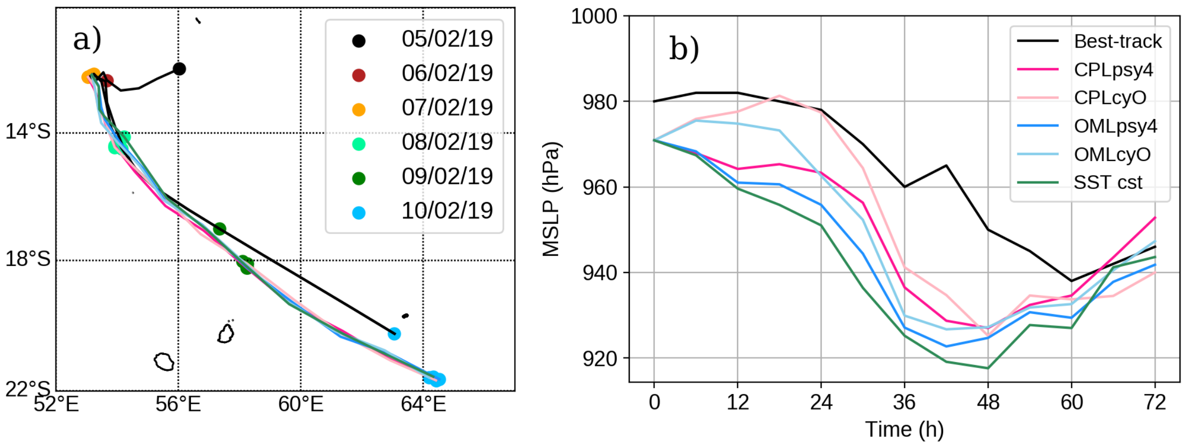

Figure 6. (a) Track of Gelena and (b) time evolution of Pmin (hPa) from the 7 February 2019 at 00 UTC till the 10 February 2019 at 00 UTC (72 h) for the RSMC La Réunion BT data (black) and the CPLpsy4 (dark pink), CPLcyO (light pink), OMLpsy4 (dark blue), OMLcyO (light blue) and SST constant (green) configurations.

Gelena has a quasi-stationary behaviour on the 6 February 2019 with an average translation speed of 1.5 m s^{-1}. On the 7 February 2019, Gelena maintains a slow translation speed of 3 m s^{-1} and then it accelerates during the next 48 h, with an average translation speeds of 8 m s^{-1}.

In the 3D coupled runs of the 6 February 2019 at 00 UTC, the cooling of the SST reaches about 6°C in the first 24 hours of the simulations. Such an intense cooling is not present in the MERCATOR product PSY4 of the 7 February 2019 at 00 UTC. The initial state of the ocean for the psy4 runs starting on the 7 February 2019 at 00 UTC is then significantly warmer than the one of the cyO runs (Figure 8(a-c)) and 9(a-c)).

Figure 6(b) shows the temporal evolution of Pmin (hPa) derived from the RSMC La Reunion BT data (black), the CPLpsy4 (dark pink), CPLcyO (light pink), OMLpsy4 (dark blue), OMLcyO (lightblue) and SST constant (green) simulations, for the runs starting on the 7 February 2019 at 00 UTC. The impact of cycling the ocean state on the TC intensity is clearly seen on the first 24 hours of the simulations as the psy4 runs are about 10 hPa deeper than the cyO runs. In this case, all runs highly overestimates the intensification after 30 h of simulation with a simulated maximum of intensity after about 36 to 48 h of simulation. At the peak of intensity, Pmin in the CPL runs is however about 5 hPa weaker than in the OML runs. The simulation with constant SST (green) shows that neglecting completely the feedback between the TC and the ocean generates in this case an even lager overestimation of maximum TC intensity of about 5 hPa compared to the OMLpsy4 simulation.

Figure 7 shows the surface (10 m) wind speeds of TC Gelena in the run starting on 7 February 2019 for the CPLcyO and OMLpsy4 simulations compared to the SAR data. The surface wind field observed by the SAR shows a maximum wind speed value in the eyewall of 37 m s^{-1} on 7 February 2019 at 02 UTC and about 35 m s^{-1} on the 8 February 2019 at 02 UTC. The winds simulated by the AROME model are much stronger than those observed by the SAR data, especially after 26 hours of simulation with OMLpsy4 when the wind speed values in the eyewall reach about 55-60 m s^{-1}. The maximum wind in CPLcyO is about 15 m s^{-1} weaker, but still more than 10 m s^{-1} higher than the observation.

The response of the ocean to the cyclonic winds in CPLpsy4, CPLcyO, OMLpsy4 and OMLcyO simulations starting on the 7 February 2019 is illustrated in Figures 8 to 11. In both CPL simulations (Figure 8(b-d)), the SST cools by an other 6°C in the first 24 h of the simulation when the TC is still slow. In OMLpsy4, the SST cools only by about 1.5°C (Figure 9b). In the OMLcyO simulation, the SST which had been cooled by 6°C in the previous coupled run now heats up by 2°C (Figure 9d). We will see later in this section that actually, in the first 12 h of simulation starting on the 7 February 2019, the OA surface fluxes in the CPLcyO and OMLcyO runs tend to heat up the ocean.

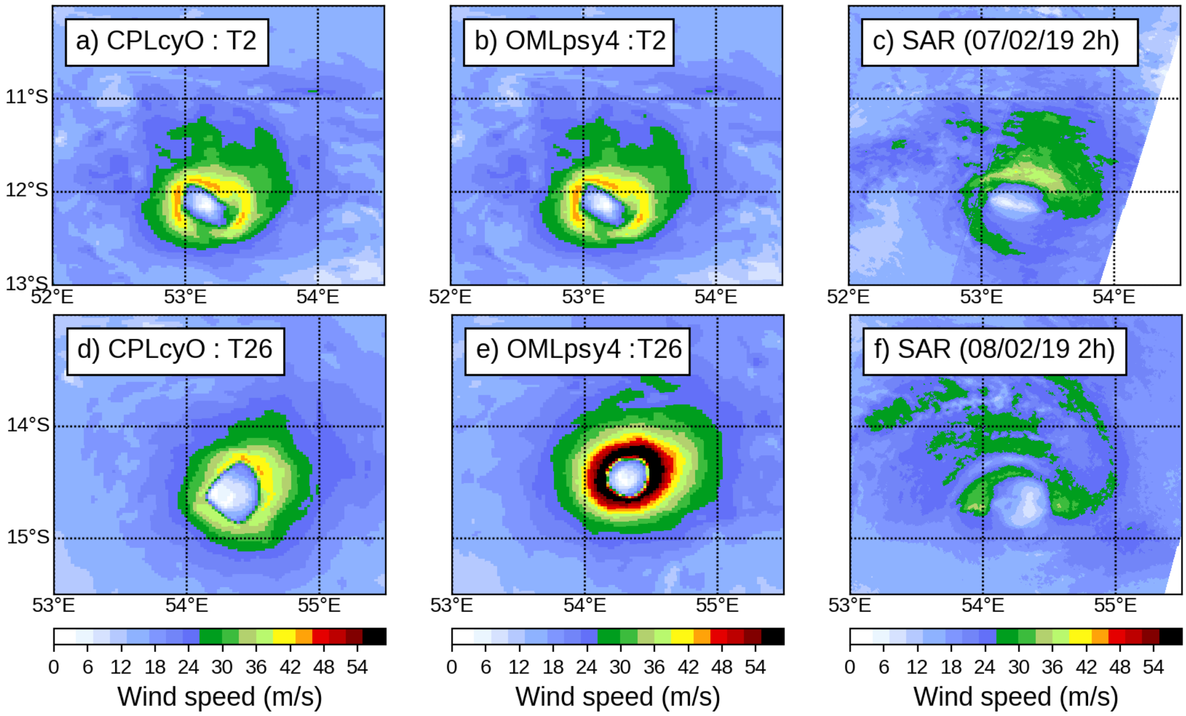

Figure 7. TC Gelena surface winds: (a-b) (resp. d-e) 10 m wind speed (m s^{-1}) of the 2 h (resp. 26 h) forecasts verifying on 7 February 2019, 02 UTC (resp. 8 February 2019, 02 UTC) for both CPLcyO and OMLpsy4; c) (resp. f) SAR surface wind speed (m s^{-1}) on 7 February 2019 at 02 UTC (resp. 8 February 2019, 02 UTC).

This difference in surface water cooling between the CPL and OML simulations is explained by the presence of an intense upwelling in the CPL runs (Figure 10). In CPLcyO, the upwelling is already intense in the initial condition. It has already crossed the bottom of the OML in the first 24 h of the previous forecast (CPLcyO from the 6 February 2019 at 00 UTC) and it remains strong in the first 24 h of the 7 February 2019 00 UTC simulation cooling the surface by an other 6°C. In the PSY4 initial condition of CPLpsy4, the upwelling is broader and weaker and still confined to 50 m below the surface At the end of the quasi-stationary period on 8 February 2019 00 UTC, the surface of the ocean is 6°C cooler in CPLcyO than in CPLpsy4.

As expected in the South hemisphere, the upwelling in the CPL runs is located on the left (East) side of the TC track. In this zone, the thermocline vanishes and the warm water of the OML is completely replaced by deeper cold water. A zone of maximum warming is observed on the East side of the cooling at a depth between 40 m and 80 m. It cor-

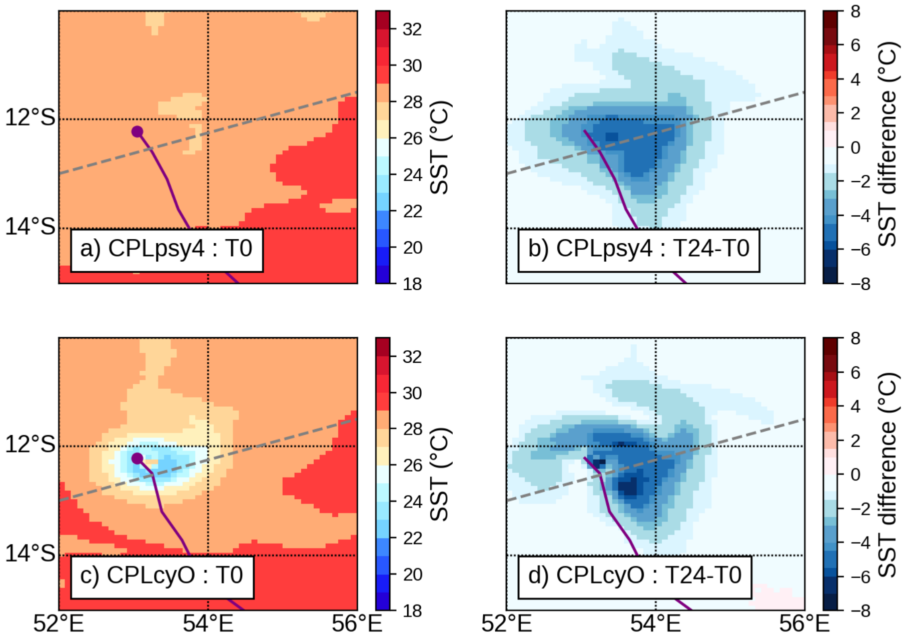

Figure 8. SST (°C) in the vicinity of Gelena for the simulation starting on the 7 February 2019 at 00 UTC : (a-c) initial condition of simulation with the CPLpsy4 (top) and CPLcyO (bottom) configurations and (b-d) SST difference (°C) between the initial condition and the 24 h forecast. The purple point gives the position of the cyclone at the time of the figure and the track of the cyclone is represented by the purple line.

responds to a zone where the turbulent mixing deepens the OML in this region as colder water originally under the initial thermocline is mixed with warmer water from the OML.

For the OMLpsy4 simulations (Figure 11), the cooling of the surface waters is very shallow, between the surface and a depth of about 20 m and it does not exceed 2°C. In OMLcyO, the intense upwelling that started in the first 24 h of the previous run cannot continue in an uncoupled run. It is slowly eroded from the top by the surface fluxes resulting in a weak warming of 1°C in the upper part of the upwelling which was present in the initial condition.

Figure 12 shows the surface latent heat fluxes (W m^{-2}) and the radial and tangential winds (m s^{-1}) at 50 m above the surface around the Gelena centre after 6 h of the simulation starting on the 7 February 2019 at 00 UTC for CPLcyO, CPLpsy4, OMLcyO and OMLpsy4. Both simulations that start with a cycled ocean show a reversal of

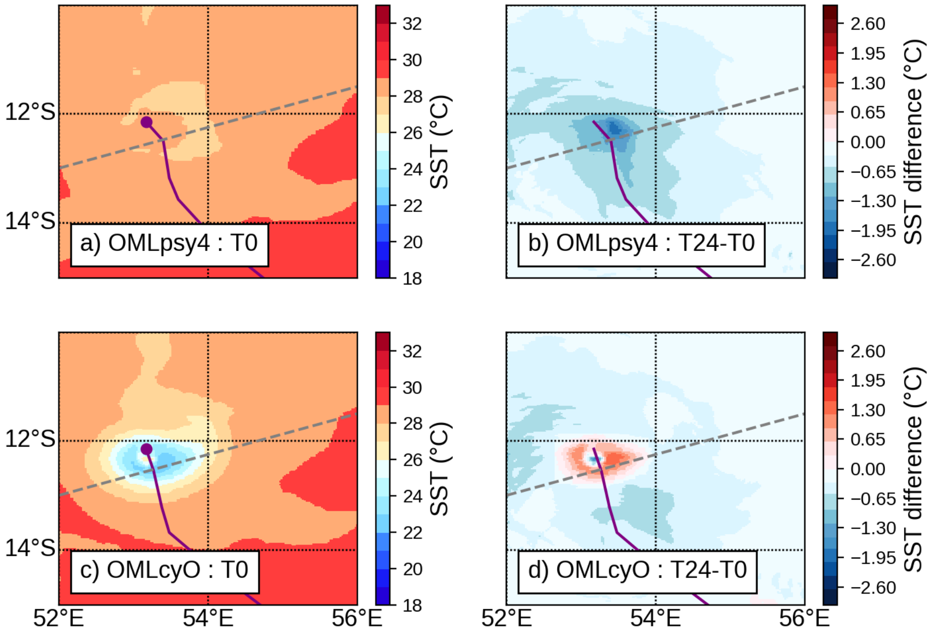

Figure 9. As Figure 8 but for OMLpsy4 and OMLcyO configurations. Note that the colour scale for the differences is different for fig. 9 and fig. 8

.

the heat fluxes at the OA interface of -250 to -500 W m^{-2} meaning that, when the ocean cooling is intense and fast, the atmosphere gives back heat to the ocean contrary to the primary mechanism leading to TC intensification. Such an inversion of sensible and latent heat fluxes between the air and the sea surface is also mentioned by Glenn et al. (2016). The minimum heat flux is observed in the left rear part of the TC track in the region of the strongest upwelling (as shown in Figure 8 and Figure 10). In OMLcyO , the inversion of heat fluxes sign under the TC (Figure 12d) causes a warming of the surface waters which is not compensated by the cooling associated with the turbulent mixing in the OML (Figures 9 and 11).

The processes below and at the surface discussed above have a direct impact on the vertical structure of the TC. Figure 13 illustrates the vertical structure of the mean state of Gelena in its NW and NE quadrants, for the CPLcyO and OMLpsy4 simulations. These two quadrants show the rear area of the cyclone where the cooling was the most intense. The strong low level convergence simulated by OMLpsy4 results in a strong con-

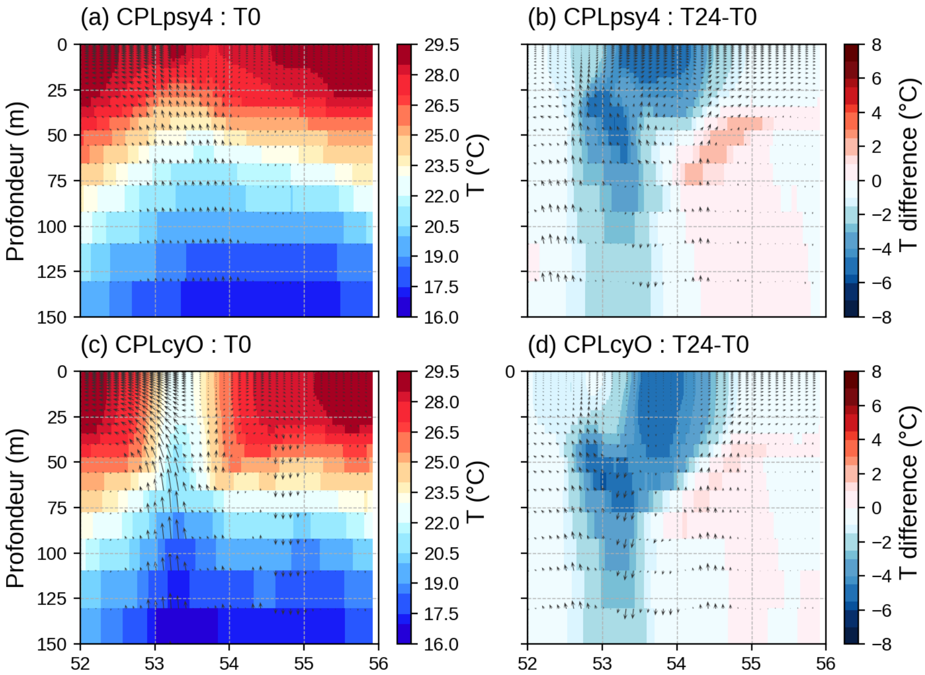

Figure 10. West-East cross-section along the dashed grey line on Figure 8 showing the evolution of the ocean temperature (T) in the run starting on the 7 February 2019 at 00 UTC run (a-c) initial condition of simulation with the CPLpsy4 (top) and CPLcyO (bottom) configurations and (b-d) temperature (T) difference (°C) between the initial condition and the 24 h forecast

vective zone, which extends up to 16 km altitude in both quadrants. In this case, the deep convection shows a circular symmetry around the eye. The maximum of synthetic radar reflectivity that is associated with the eyewall extends up to 5 km above the surface. In CPLcyO, the convergent secondary circulation at the surface is weaker. The depth of the deep convection is reduced to 14 km height. In this case, the cyclone is more asymmetric with weaker convection in the NE part above the coldest surface waters. Low level clouds forms in the northern part of the eye where the heat fluxes are negative (Figure 13) while in OMLpsy4, the TC eye remains very dry. Low level clouds in the eye are a well known feature (see for example, Kossin et al., 2002 and Houze, 2010), but to our knowledge, their formation has not yet been linked to the ocean cooling under a TC.

In summary for the case of Gelena, all 5 model configurations overestimate the TC intensity. In the operational configuration OMLpsy4, the maximum wind near the max

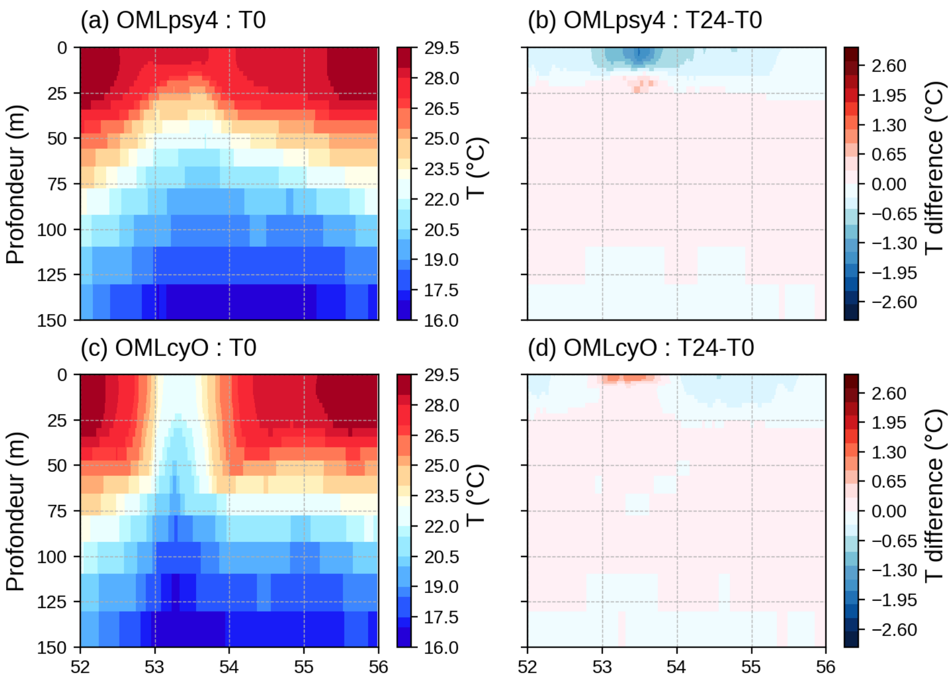

Figure 11. As Figure 10 but for OMLpsy4 and OMLcyO configurations. Note that the colour scale for the differences is different for fig. 11 and fig. 10.

of intensity is about twice the observed wind speed. The overestimation is reduced by a factor of two in the CPLcyO configuration. The feedback between the upwelling and the TC which is present only in the coupled configurations is a key factor in this case where the TC remains quasi-stationary for almost 48 h. But, if the coupling with a 3D ocean model partially solves the overestimation of the winds, other components of the model are probably still needed to improved the behaviour of the model in the case of intense TC (surface flux parameterization, coupling with waves/sea sprays, currents, cloud microphysics). This case also shows the importance of the choice of oceanic initial condition in short term forecasts. The memory of the oceanic circulations triggered by the high resolution TC winds from AROME is lost if the ocean in the coupled model is initialised by the PSY4 products. The impact on the TC intensity is found to be significant in case of intense cooling.

In the case of Gelena, we could not find any in situ measurements to validate the SST cooling. It is then impossible to conclude on the realism of the 12°C cooling in 48 hours produced by the CPLcyO configuration. References to such large cooling are found

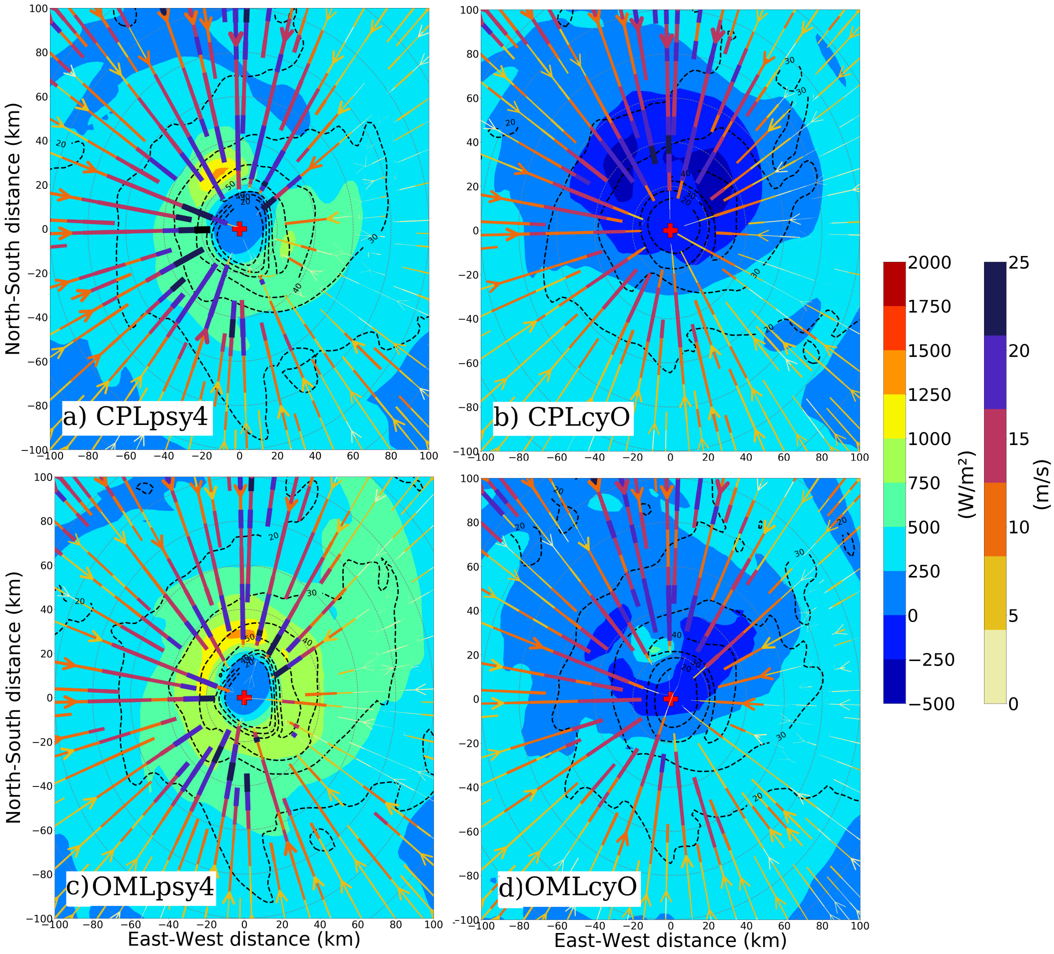

Figure 12. Surface latent heat fluxes (W m^{-2}, shading) near the centre of Gelena after 6 h of simulation of runs starting on the 7 February 2019 at 00 UTC : a) CPLpsy4, b) CPLcyO, c) OMLpsy4 and d) OMLcyO. The radial wind at 50 m above the surface (m s^{-1}) is represented by the coloured arrows and isolines of tangential wind speed (m s^{-1}) are drawn with black dashed contours.

in the literature (Chiang et al., 2011; Guan et al., 2021). Our belief is however that the ocean cooling that is obtained by the CPLcyO configuration in the case of Gelena is a bit overestimated as a consequence of the overintensification of the TC intensity in AROME-NEMO.

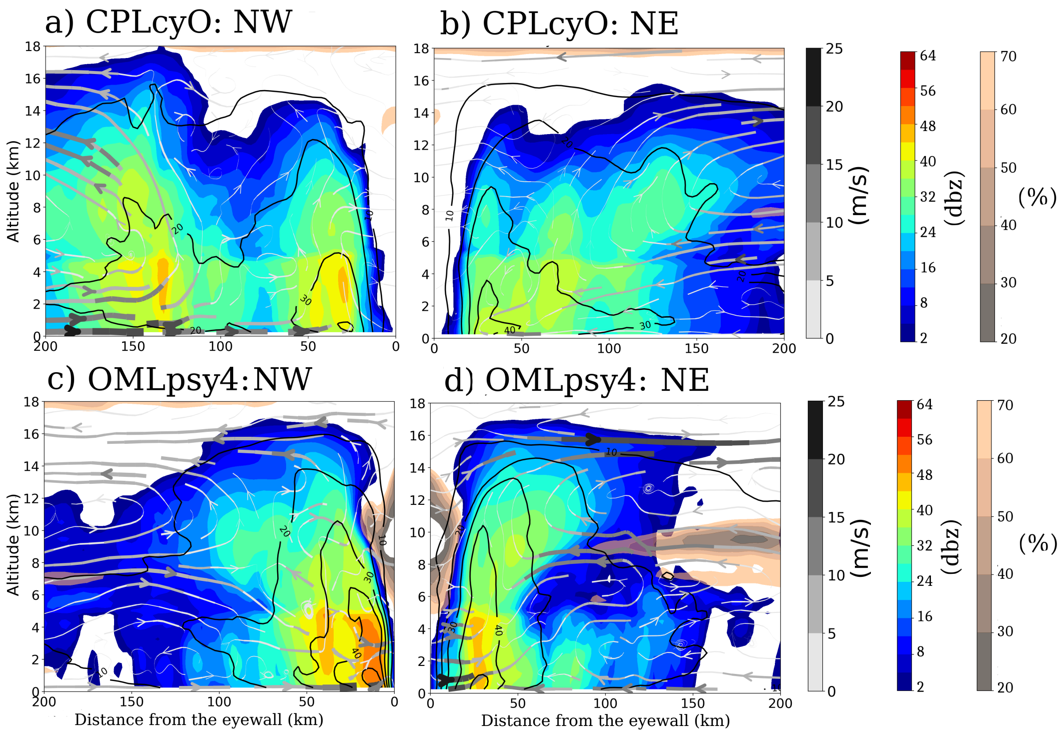

Figure 13. Vertical sections of the azimuthal mean of synthetic radar reflectivity (dBz) for the (a-c) North-West and (b-d) North-Est quadrants of Gelena after 12 h of simulation from the 7 February 2019 at 00UTC with the OMLpsy4 and CPLcyO configurations. On the same figure, the secondary circulation is shown with streamlines in black and white and the tangential wind speed (m s^{-1}) with black isocontours. Relative humidity (%) is in pink/grey shadings.

3.3 Belna: a case of steadily moving TC

3.3.1 Belna analysis by the RMSC-La Réunion

Belna developed within a low level convergence zone resulting from the conjunction of a Madden Julian oscillation phase and the passage of an equatorial Rossby wave in early December 2019 South of the Seychelles. During the night of 05 December, it developed from a moderate to a STS and became a TC on the morning of 07 December. Belna reached its maximum intensity in the late afternoon of 7 December with maximum estimated winds of 43 m s^{-1} and a minimum sea level pressure of 954 hPa. It maintained a south-western track and passed between the islands of Aldabra and Astove and 100 km west of Mayotte during the day on 08 December. It weakened to a STS during the first six hours of 09 December, and then re intensified to a TC during the next six hours north of Madagascar. During the following days, Belna weakened and it completely dissipated on 11 December.

TC Belna was not moving very fast, but it has a regular pace at about 4 m s^{-1}. In enters the AROME domain during the night of 5 December. We will focus on the run starting on the 6 February 2019 at 00 UTC. In this case, the initial oceanic state from PSY4 and from the cycled ocean configurations are very similar.

3.3.2 Simulations of TC Belna

In this section, the development of TC Belna and the corresponding response of the ocean are analysed with a set of 5 runs starting on the 6 December 2019 at 00 UTC.

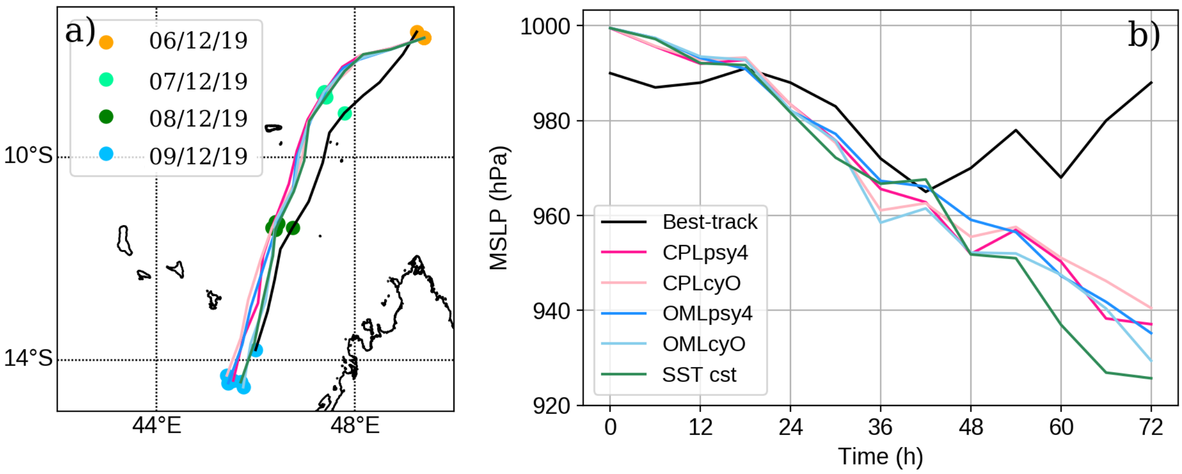

Figure 14. (a) Track of Belna and (b) Time evolution of Pmin (hPa) from the 06 December 2019 at 00 UTC to the 9 December 2019 at 00 UTC (72 h) for the RSMC La Réunion BT data (black) and the CPLpsy4 (dark pink), CPLcyO (light pink), OMLpsy4 (dark blue), OMLcyO (light blue) and SST constant (green) configurations.

Figure 14 shows the track of Belna and the time evolution of Pmin (hPa) as given by the RSMC La Reunion BT data (black) and derived from the CPLpsy4 (dark pink), CPLcyO (light pink), OMLpsy4 (dark blue), OMLcyO (lightblue) and SST constant (green) simulations. As in the case of TC Gelena, Belna tracks are very similar in the 5 simulations (Figure 14a) and they are close to the BT (black line), with a small westward error in TC position in the first 48 h of the simulations. The average error is about 60 km over the entire period. The simulated translation speed of Belna is on average 4 m s^{-1} during the whole simulation (not shown). During the first 36 hours, the Pmin forecast in the 5 configurations remains close to the BT analysis. But after 36 h, the TC continues to intensify in all model configurations while Belna starts to weaken in the observations.

The anomaly in the forecast is confirmed by the comparison with two SAR images (Figure 15). After 26 hours of simulation, the wind speed values in the eyewall are very similar to those observed on the SAR images, i.e. between 30 and 40 m s^{-1}. However, after 50 h of simulation, a few hours after the intensity peak, the wind speeds in the eyewall are about 30 m s^{-1} higher in the CPLcyO and OMLpsy4 simulations than in the SAR data.

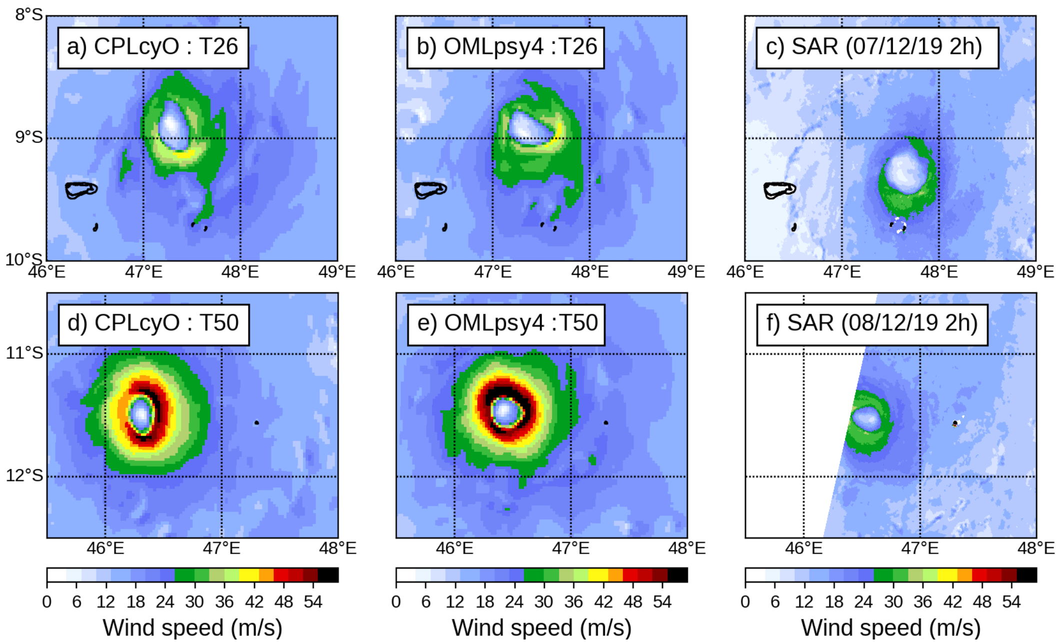

Figure 15. TC Belna surface winds: (a-b) (resp. d-e) 10 m wind speed (m s^{-1}) of the 26 h (resp. 50 h) forecasts verifying on 7 December 2019, 2 UTC (resp. 8 December 2019, 2 UTC) for both CPLcyO and OMLpsy4; c) (resp. f) SAR surface wind speed (m s^{-1}) on 7 December 2019 at 2 UTC (resp. 8 December 2019, 2 UTC).

The response of the ocean in CPLcyO and OMLpsy4 simulations starting on the 6 December 2019 is illustrated in Figure 16 and figure 17. CPLpsy4 (resp. OMLcyO) is not shown because the results are very similar with CPLcyO (resp. OMLpsy4). The

CPLcyO and OMLpsy4 simulations start with very similar oceanic states (Figure 16a and c). After 48 hours of simulation, in both CPLcyO and OMLpsy4 the area of SST cooling around the TC is quite large, on both side of the track. The maxima of cooling are however still found on the left (East) side of the track, with a maximum value of 2°C in CPLcyO and OMLpsy4. The vertical cross-section shown in Figure 17 show a narrow upwelling in the CPL run which weaken as it reaches the bottom of the OML. Most of the cold water remains confined under the OML at around 50 m depth. A weak extension of upwelling in the OML may however explain the small difference in SST cooling between the CPLcyO and the OMLpsy4 runs. In this case, the upwelling does not destroy the thermocline, but the depth of the thermocline gains about 20 m in the vicinity of the TC as indicated by the positive temperature tendencies between 50 and 70 m in Figure 17(b-d).

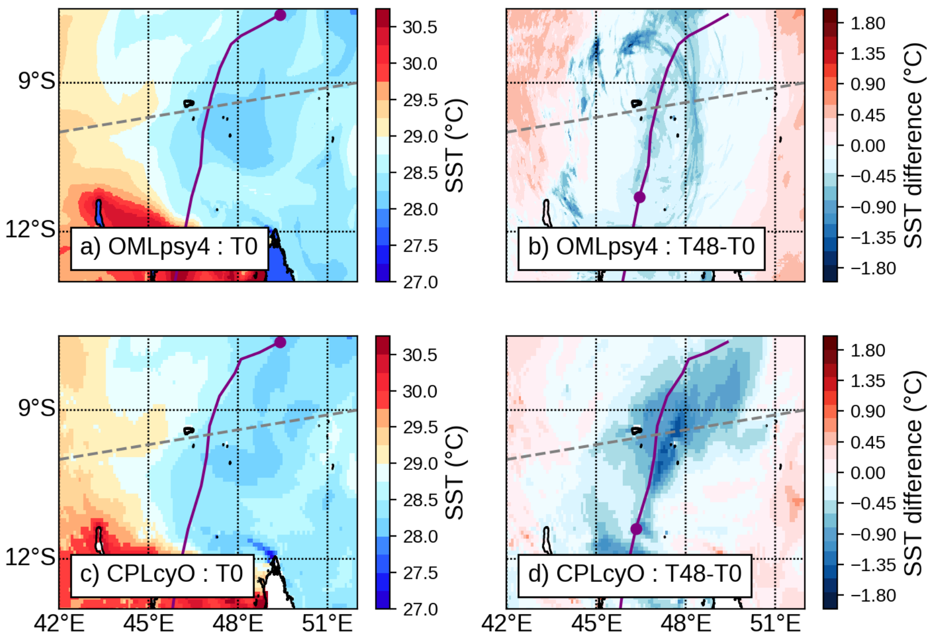

Figure 16. SST (°C) in the vicinity of Belna for the simulation starting at 00 UTC on the 6 December 2019 : (a-c) initial condition of simulation with the OMLpsy4 (top) and CPLcyO bottom) configurations and (b-d) SST difference (°C) between the initial condition and the 48 h forecast. The purple point gives the position of the cyclone at the time of the figure and the track of the cyclone is represented by the purple line.

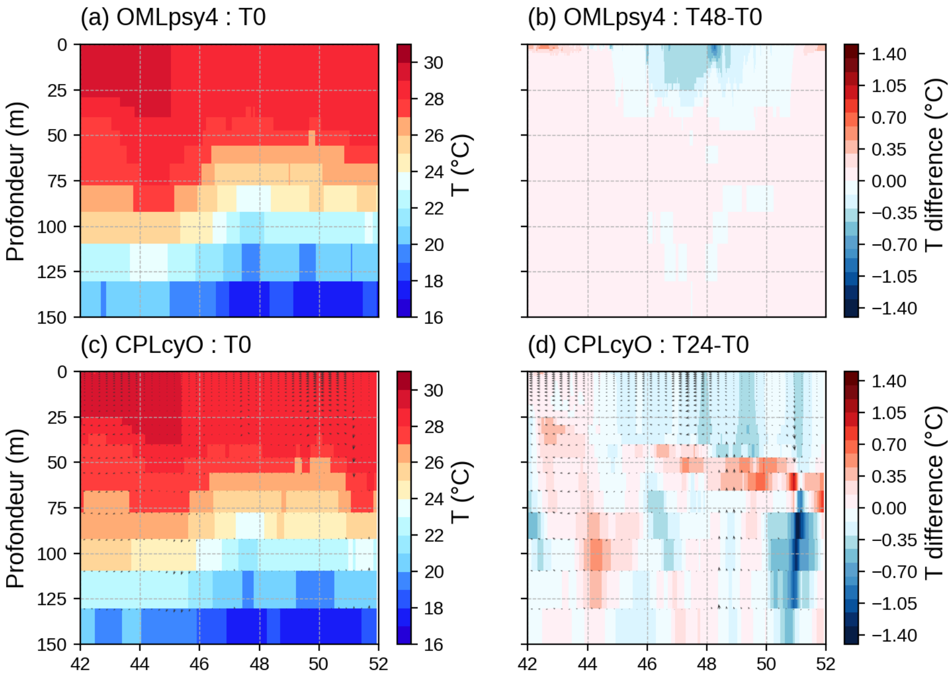

Figure 17. West-East cross-section along the dashed grey line on Figure 16 showing the evolution of the ocean temperature (T) in the run of the 6 December 2019 at 00 UTC (a-c) initial condition of simulation with the OMLpsy4 (top) and CPLcyO (bottom) configurations and (b-d) temperature (T) difference (°C) between the initial condition and the 48 h forecast

In the case of Belna, the impact of the 3D coupling with the ocean is limited. In particular, the lack of coupling was not responsible for the large intensity estimation in the last 36 h of the operational forecast starting on the 6 December 2019 at 00 UTC. The reason of this intensity error has yet to be understood with future works.

3.4 Batsirai: a case with buoy observations

We present here an analysis of TC Batsirai, which developed into a category 4 TC during the 2021-2022 TC season of the SWIO, and for which in situ buoy observations are available, unlike TCs of the previous three seasons. For this case, we mainly focus on the comparison of the oceanic state of the CPLcyO and OMLpsy4 experiment with the buoy measurements, taking advantage of such a rare opportunity in the SWIO basin to validate the evolution of the SST in the model in the vicinity of a TC with good quality measurements.

3.4.1 Batsirai analysis by the RMSC-La Réunion

Batsirai was the second tropical system and the first to reach the TC level of the 2021-2022 cyclone season in the SWIO. It formed within a very active monsoon trough on the 24 January 2022 in the northeast of the SWIO basin at the edge of a trans-equatorial monsoon flow. After a short phase of rapid intensification on 27 January, Batsirai weakens over the following days as it encounters larger wind shear and dry air intrusions along its westward track. On 29 January, it meets much more favourable conditions and re-intensifies into a Category 4 hurricane. As it travels north of Mauritius on 31 January, it causes heavy flooding on the Island of St Brandon because of the combined effect of a storm surge and a swell with the largest waves estimated between seven and nine meters. Batsirai becomes an ITC on 2 February as it is the closest to La Réunion. Winds exceeded 42 m s^{-1} in the highest ridges of La Réunion. Exceptional rainfall of about 1500 mm have been recorded on the volcano area during this episode. The storm underwent an eyewall replacement the following day and fluctuated in intensity before making landfall on the East coast of Madagascar on 5 February as a category 3 cyclone causing at least 121 casualties and a lot of damages on housing and infrastructures. The system then weakened quickly as it crossed Madagascar. It emerged as a TS between Mozambique and southern Madagascar on 7 February, and then became a post-tropical depression on 8 February.

3.4.2 Comparison of TC Batsirai simulations with buoy measurements and SAR winds

As it is often the case in an operational context, the NWP guidances for TC tracks and intensities are not perfect, but they still remain a valuable source of information for the RSMCs. As Batsirai was at its closest from La Réunion, the uncertainty in the track forecast was still large both in cross track and along track direction in most NWP models. AROME overestimated the speed of displacement and the Southward curvature of Batsirai track. For the more detailed discussion below, we have selected the 48 h run from the 3 February 2022 at 00 UTC as it covered the period when the TC displacement is the slowest. With the criteria used for the TC of the 2018-2019 and 2019-2020 seasons in the previous sections, Batsirai would be classified as a slow cyclone during this 48 h period.

The initial intensity of the TC in AROME-IO is underestimated after the 6-h warmup (Figure 18a). In the operational configuration OMLpsy4 from the 3 February 2022 at 00 UTC, the TC rapidly intensify and overtake the observed intensity after 12 hours of simulation (Figure 18b). In the coupled run CPLcyO, the intensification is weaker (Figure 18) but the winds in the eyewall after 39 h of simulation are nevertheless 2-3 m s^{-1} stronger than the estimation given by the SAR wind retrieval (Figure 19). At the time of the SAR observation, the asymmetry of the system with weaker winds in the North-East quadrant is better seen in the coupled simulation than in the operational configuration.

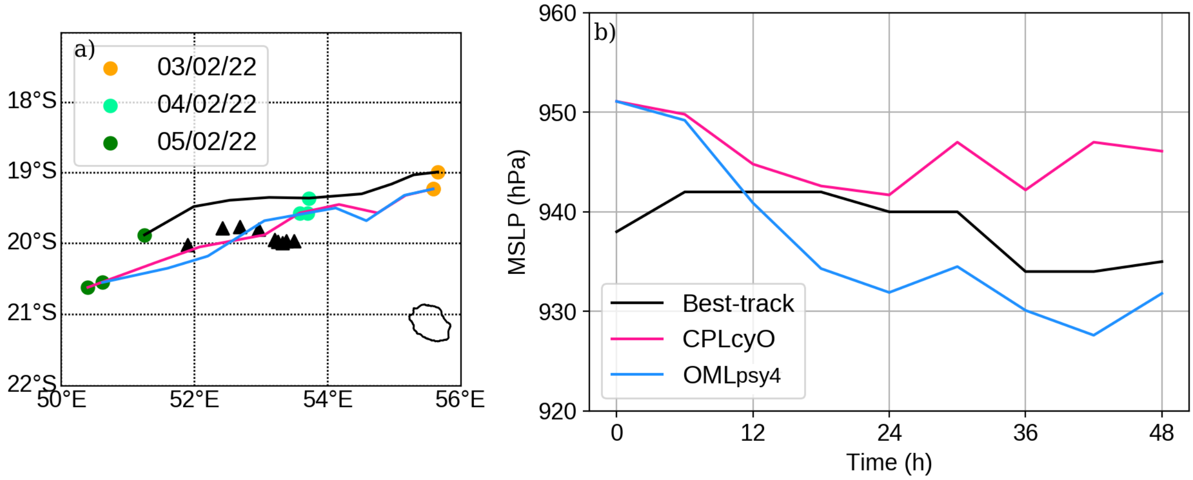

Figure 18. (a) Track of Batsirai and (b) Time evolution of Pmin (hPa) from the 3 February 2022 at 00 UTC to the 5 February 2022 at 00 UTC (48 h) for the RSMC La Réunion BT data (black) and the CPLpsy4 (pink) and OMLpsy4 (blue) configurations. The black triangles show the position of a drifting buoy every 6 h between the 3 and the 5 February 2022.

TC Batsirai triggers a SST cooling North of the Mascarene Islands when it displacement velocity is at its slowest. In the cold wake on the South side of Batsirai track simulated by CPLcyO configuration, the maximum cooling is about 4°C (Figure 20). In the OMLpsy4, it is only about 1°C.

Figure 21 shows the evolution of the SST measured by the drifting buoy indicated by a black triangle on Figure 20 (black line). The SST at the buoy loses about 3°C between the 3 February 2022 at 00 UTC and the 5 February 2022 at 00 UTC. The pink curves on Figure 21 show the evolution of the SST at the position of the buoy in three

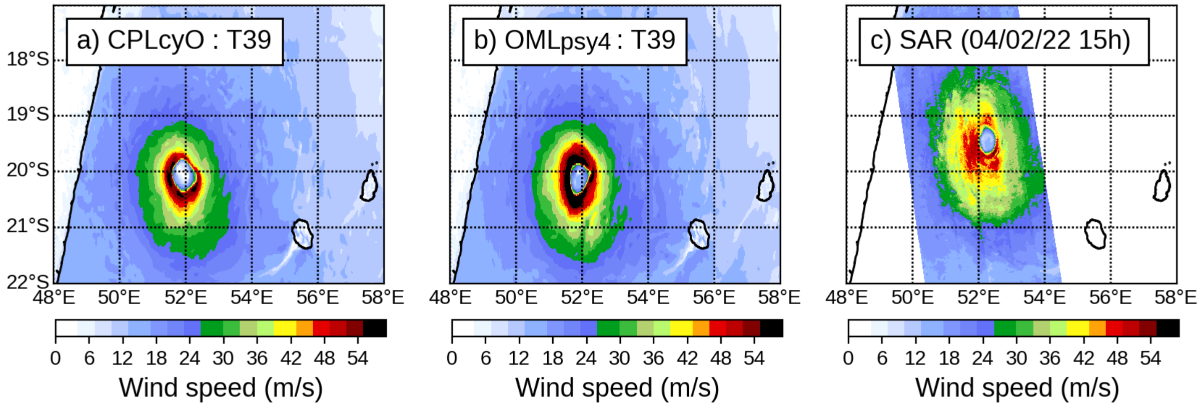

Figure 19. TC Batsirai surface winds: (a-b) 10 m wind speed (m s^{-1}) of the 39 h forecasts verifying on 4 February 2022, 15 UTC for both CPLcyO and OMLpsy4 c) SAR surface wind speed (m s^{-1}) on 4 February 2022 at 15h.

successive CPLcyO runs (2 February at 00UTC, 3 February at 00UTC and 4 February 2022 at 00 UTC). AROME-NEMO reproduces a very similar evolution of the SST but with an advance of about 24 h. The error in the track position, and especially the along track error that results from an overestimation of the TC translation velocity is a likely reason for the timing error of the SST cooling in the model in this case.

This last case illustrates well the difficulty of the comparison of TC simulations with observations, especially when there is an error in the TC position forecast. However, the confrontation of the buoy observations with the result of the CPLcyO simulation shows that the oceanic response of the coupled system AROME-IO/NEMO is realistic when the surface winds of the TC are close to the observed values.

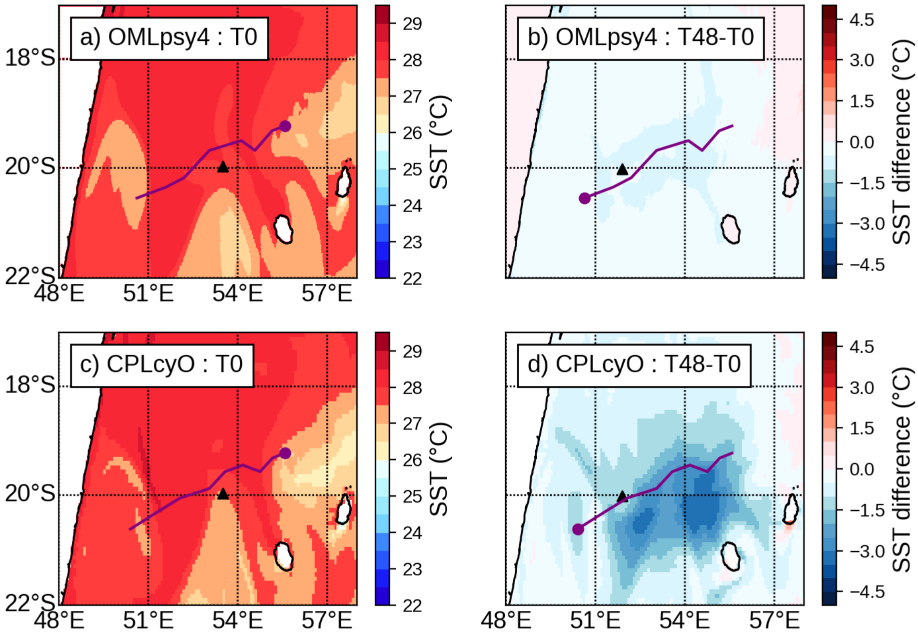

Figure 20. SST (°C) in the vicinity of Batsirai for the simulation starting at 00 UTC on the 3 Februrary 2022 : (a-c) initial condition of simulation with the OMLpsy4 (top) and CPLcyO bottom) configurations and (b-d) SST difference (°C) between the initial condition and the 48 h forecast. The purple point gives the position of the cyclone at the time of the figure and the track of the cyclone is represented by the purple line. The black triangle show the position of the drifting buoy.

4 Discussion and conclusion

The overseas version of the convection-permitting numerical weather prediction model AROME-IO which is used by the RSMC-cyclones of La Réunion, is coupled every 5 minutes to a 1D parameterization of the OML. The present study aimed at testing the replacement of the simplified OA interaction described by the 1D parameterization of the OML by a full 3D coupling with the oceanic model NEMO in a future configuration of AROME-IO. The implementation of the coupled configuration AROME-IO/NEMO which was the first step needed for this study has then been facilitated by the developments which had already been made in the surface platform SURFEX used by AROME. The data exchange between the atmosphere and the ocean is managed by the OASIS coupler every hour. Unlike the 1D parameterization, the ocean model needs boundary con-

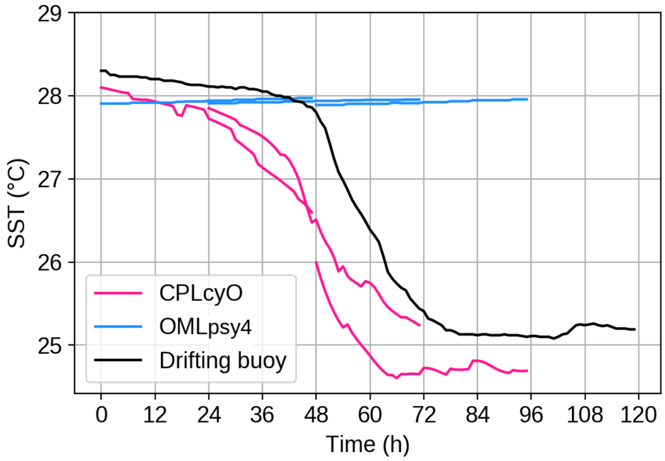

Figure 21. Time evolution of the SST (°C) measured by drifters in the vicinity of Batsirai track (black line). Comparison with SST at the location of the drifters in 3 successive 48 h simulations starting on the 2 February, 3 February and 4 February 2022 at 00UTC, with the CPLcyO configuration (pink) and the OMLpsy4 configuration (blue).

ditions which are prepared from the global oceanic products of MERCATOR-Ocean. In the design of the coupled system, we kept in mind the constraints imposed by a future operational system. For example, we only used data sources which would be available in real time. Early on in the design process, the question of the initialisation of the ocean has been raised for the case of a forecast system running 4 times a day for short forecasts (48 to 78 hours). Several solutions have been tested and two of them have been selected for the analyses presented in this article.

Atmospheric and oceanic in situ observations in the vicinity of TCs are very sparse in the IO. High resolution satellite wind measurements are irregular and SST products are of low quality due to cloud cover. Unlike in the Atlantic or North Pacific basin, it is difficult to validate NWP configuration against observation. The validation of TC forecast is then often limited to the comparison of macroscopic characteristics such as position, minimum of pressure at the centre of the TC and maximal wind. In a few cases, high resolution SAR images and buoys measurement give useful information for model evaluation.

The main results of this study are based on a comparison between five configurations of AROME-IO; one with constant SST, two with the coupled AROME-NEMO model and two with the OML parameterization. For each of these two OA coupling options, the initial condition of the ocean is either directly interpolated from the MERCATOR-Ocean PSY4 products as it is the case for the initialisation of the OML in the current operational model or it is cycled by the AROME-NEMO system since a few days before the cyclone intensification. Three-day forecasts for about 30 starting dates and 7 different TCs of the 2018-2019 and 2019-2020 TC cyclone seasons have been produced. The simulations are first compared with classical scores against the RSMC BT data. Then, case studies illustrate the differences between the different coupling solution for a selection of 3 TCs.

The scores shows that:

- there is very little impact of the 3D coupling on the TC track. This was expected as, in a limited area model, the track is mainly driven by the larger scale of the host model.
- there is an improvement of the cyclone intensity forecast with the 3D coupling in AROME-IO both in terms of bias and standard deviation. These improvements are particularly true for TCs that encounter a slow propagation phase (less than 2 m s^{-1} for at least 12 hours).
- the memory of the mesoscale OA interaction also contributes to better TC intensity in the first 36 h of the forecast, both for 3D coupling and 1D OML parameterization.

These results are confirmed by the 3 case studies. The detailed analyses of the OA interaction also show that:

- very intense winds in a stationary TC may trigger strong upwelling which are cooling the ocean surface of more than 5°C per day. In such extreme cases, the OA thermodynamic fluxes are reversed compared to the usual TC configuration where the ocean fuels the TCs. The TC intensification is then significantly affected. Intense coolings modify the structure of the boundary layer, both in the wall and in the eye, with possible formation of low level clouds in the eye.
- the 3D upwellings are deep circulations which affect first the bottom of the OML. The strongest upwelling will completely modify the structure of the OML and the well mixed water will be replaced by cold water advected upward across the ther-

mocline. In case of regularly moving TC, weak upwellings are triggered; colder water accumulates under the thermocline and slowly mixes with the upper layer. The feedback on the TC intensity is then weak as the maximum cooling is weaker and anyway, the TC is not affected by the maximum cooling as it has moved on.

Even if the 3D coupling reduces the tendency of AROME-IO to over intensify already intense cyclones, the scores against the BT and the case studies show that the limitation of the simplified 1D coupling with the ocean is only one aspect of the problem.

One other avenue to control the TC intensification is to improve the parameterization of the surface fluxes in case of strong winds. In the ECUME "bulk" parameterization of the surface fluxes above the ocean currently used in AROME, the momentum flux decreases for winds larger than 30 m s^{-1} and then levels off for larger wind speeds. However, there is no real consensus about the behaviour of the momentum and heat fluxes for very strong winds (and almost no measurements). A possibility would be to move from a strongly parameterize "bulk" scheme as ECUME towards a scheme with more degrees of freedom. We are currently testing the WASP scheme (Wave-Age Stress dependent Parameterization; Sauvage et al., 2020) which has recently been implemented in SURFEX. WASP is based on the COARE3.0 (Fairall et al., 2003) and COARE 3.5 (Edson et al., 2013) schemes. It offers the possibility to explicitly account for the wave growth in the calculation of the roughness length at the wind range where the momentum of the atmosphere transferred to the waves is between 7 and 25 m s^{-1}. Above 25 m s^{-1}, the contribution of wave breaking is dominant and the wave age is no longer a sufficient parameter to represent the impact of the sea state on the surface roughness. The contribution of sea sprays to the OA exchanges in case of high winds is also probably to be considered. Several ongoing researches on this topics may contribute to further improvement of the air-sea exchange parameterization in TC conditions.

A second avenue would be to work on the microphysics scheme. The ICE3 microphysics currently used in AROME is a 1 moment microphysics without any direct feedback on aerosol concentration. Tests with a 2 moment microphysics have shown that a prognostic concentration in marine and dust aerosol limits the TC growth (T. Hoarau et al., 2018). However, the introduction of new degrees of freedom in the system brings new sources of uncertainty and should then be very carefully evaluated in a prospective of operational use. The initialisation and the lateral boundary coupling of the aerosol and the parameterization of the sources of aerosol are also factors that must be of sufficient quality for the performance of the models to improve.

AROME-NEMO is an evolution toward a more realistic regional forecast system for TCs. With a resolution of 1/12 of a degree, the computational cost of the ocean model NEMO remains negligible compared to the cost of the atmospheric model AROME. There is however a clear increase in the complexity of the forecast suite as the suite needs to prepare the initial and lateral boundary conditions for NEMO and the data to feed the OASIS coupler at the beginning of the simulation.

This study also illustrates the importance of the ocean initial conditions in a coupled NWP suite. We have found that the MERCATOR PSY4 products which are currently forced by winds with a native resolution of about 10 km show a much weaker response in term of upwelling (but also in term of quasi-inertial waves; G. Hoarau & Malardel, 2021) than what we have found in the coupled AROME-NEMO configuration. Our results show that a suite where the ocean model is initialised every 24 hours by a new PSY4 ocean state looses the memory of the TC high resolution wind forcing. We have also shown that the memory of the high wind forcing can be kept if the ocean state from a previous forecast is used to initialised the next forecast. However, in an operational suite, the ocean cannot be cycled indefinitely without any correction towards oceanic observation. It is then important to implement a solution which combine the PSY4 ocean state which is regularly updated by an oceanic data assimilation and a previous forecast of the ocean which has seen high resolution winds. Several solutions from a simple linear relaxation toward the PSY4 state to more scale selective nudging procedures will be tested.

In this study, we made the choice to use the same atmospheric initial condition for all the experiments in order to focus on the sensitivity to the oceanic component and the coupling solution. But an effort to improve the initial balance between the atmosphere and the ocean in the initial conditions of both fluids will be needed. The simplest solution will be to adapt the warmup procedure which is currently used for the atmosphere to reduce the initial spin-up of the downscaling adjustment of the IFS fields to the AROME resolution to the coupled configuration. In parallel, research and development activities towards a coupled data assimilation system for AROME are starting in the research groups at Météo-France.

Acknowledgments

This work was supported by a PhD grant from Météo-France.

Availability Statement

The atmospheric model used in this study is AROME Cycle 43t2 which has been the operational version of the AROME-overseas from July 2019 to June 2022. The ocean model is NEMO, version 3.6. The atmospheric and the oceanic models are coupled with the OASIS3-MCT coupler.

The SAR data have been uploaded from https://cyclobs.ifremer.fr/app/ and the data from the ARGO drifters from http://www.coriolis.eu.org/Data-Products/Data-selection.

The Best Track data have been extracted from the Best Track data base of the Direction Régional de l'Océan Indien (DIROI) of Météo-France. These data are shared with the IBTracs data base (https://www.ncdc.noaa.gov/ibtracs/) after a subjective reanalysis by the DIROI forecasters at the end of each TC season.

References

Amante, C., & Eakins, B. W. (2009). *Etopo1 global relief model converted to panmap layer format* [data set]. PANGAEA. Retrieved from `https://doi.org/10.1594/PANGAEA.769615` doi: 10.1594/PANGAEA.769615

Bao, J., Wilczak, J., Choi, J., & Kantha, L. (2000). Numerical simulations of air–sea interaction under high wind conditions using a coupled model: A study of hurricane development. *Monthly Weather Review*, *128*(7), 2190–2210.

Belamari, S. (2005). Report on uncertainty estimates of an optimal bulk formulation for surface turbulent fluxes. *Marine EnviRonment and Security for the European Area–Integrated Project (MERSEA IP), Deliverable D*, *4*, 505.

Bender, M. A., Ginis, I., & Kurihara, Y. (1993). Numerical simulations of tropical cyclone-ocean interaction with a high-resolution coupled model. *Journal of Geophysical Research: Atmospheres*, *98*(D12), 23245–23263.

Bender, M. A., Ginis, I., Tuleya, R., Thomas, B., & Marchok, T. (2007). The operational gfdl coupled hurricane–ocean prediction system and a summary of its performance. *Monthly Weather Review*, *135*(12), 3965–3989.

Bielli, S., Barthe, C., Bousquet, O., Tulet, P., & Pianezze, J. (2021). The effect of atmosphere–ocean coupling on the structure and intensity of tropical cyclone bejisa in the southwest indian ocean. *Atmosphere*, *12*(6), 688.

Black, P. G. (1983). *Ocean temperature changes induced by tropical cyclones.* The Pennsylvania State University.

Bloom, S., Takacs, L., Da Silva, A., & Ledvina, D. (1996). Data assimilation using incremental analysis updates. *Monthly Weather Review*, *124*(6), 1256–1271.

Bougeault, P., & Lacarrere, P. (1989). Parameterization of orography-induced turbulence in a mesobeta–scale model. *Monthly weather review*, *117*(8), 1872–1890.

Bouin, M.-N., & Lebeaupin Brossier, C. (2020). Surface processes in the 7 november 2014 medicane from air–sea coupled high-resolution numerical modelling. *Atmospheric Chemistry and Physics*, *20*(11), 6861–6881.

Bousquet, O., Barbary, D., Bielli, S., Kebir, S., Raynaud, L., Malardel, S., & Faure, G. (2020). An evaluation of tropical cyclone forecast in the southwest indian ocean basin with arome-indian ocean convection-permitting numerical weather predicting system. *Atmospheric Science Letters*, *21*(3), e950.

Chang, S. W., & Anthes, R. A. (1978). Numerical simulations of the ocean's nonlinear, baroclinic response to translating hurricanes. *Journal of Physical Oceanography*, *8*(3), 468–480.

Chiang, T.-L., Wu, C.-R., & Oey, L.-Y. (2011). Typhoon kai-tak: An ocean's perfect storm. *Journal of Physical Oceanography*, *41*(1), 221–233.

Courtney, J. B., Langlade, S., Barlow, S., Birchard, T., Knaff, J. A., Kotal, S., ... others (2019). Operational perspectives on tropical cyclone intensity change part 2: Forecasts by operational agencies. *Tropical Cyclone Research and Review*, *8*(4), 226–239.

Craig, A., Valcke, S., & Coquart, L. (2017). Development and performance of a new version of the oasis coupler, oasis3-mct_3. 0. *Geoscientific Model Development*, *10*(9), 3297–3308.

Edson, J. B., Jampana, V., Weller, R. A., Bigorre, S. P., Plueddemann, A. J., Fairall, C. W., ... Hersbach, H. (2013). On the exchange of momentum over the open ocean. *Journal of Physical Oceanography*, *43*(8), 1589 - 1610. Retrieved from `https://journals.ametsoc.org/view/journals/phoc/43/8/jpo-d-12-0173.1.xml` doi: 10.1175/JPO-D-12-0173.1

Fairall, C. W., Bradley, E. F., Hare, J. E., Grachev, A. A., & Edson, J. B. (2003).

Bulk parameterization of air–sea fluxes: Updates and verification for the coare algorithm. *Journal of Climate*, *16*(4), 571 - 591. Retrieved from `https://journals.ametsoc.org/view/journals/clim/16/4/1520-0442_2003_016_0571_bpoasf_2.0.co_2.xml` doi: 10.1175/1520-0442(2003)016⟨0571:BPOASF⟩2.0.CO;2

Faure, G., Chambon, P., & Brousseau, P. (2020). Operational implementation of the arome model in the tropics: Multiscale validation of rainfall forecasts. *Weather and Forecasting*, *35*(2), 691–710.

Feng, X., Klingaman, N. P., & Hodges, K. I. (2019). The effect of atmosphere–ocean coupling on the prediction of 2016 western north pacific tropical cyclones. *Quarterly Journal of the Royal Meteorological Society*, *145*(723), 2425–2444.

Gaspar, P., Grégoris, Y., & Lefevre, J.-M. (1990). A simple eddy kinetic energy model for simulations of the oceanic vertical mixing: Tests at station papa and long-term upper ocean study site. *Journal of Geophysical Research: Oceans*, *95*(C9), 16179–16193.

Ginis, I. (2002). Tropical cyclone-ocean interactions. *Advances in Fluid Mechanics*, *33*, 83–114.

Glenn, S., Miles, T., Seroka, G., Xu, Y., Forney, R., Yu, F., … Kohut, J. (2016). Stratified coastal ocean interactions with tropical cyclones. *Nature communications*, *7*(1), 1–10.

Guan, S., Zhao, W., Sun, L., Zhou, C., Liu, Z., Hong, X., … Hou, Y. (2021). Tropical cyclone-induced sea surface cooling over the yellow sea and bohai sea in the 2019 pacific typhoon season. *Journal of Marine Systems*, *217*, 103509.

Haiden, T., Janousek, M., Bidlot, J., Buizza, R., Ferranti, L., Prates, F., & Vitart, F. (2018). *Evaluation of ecmwf forecasts, including the 2018 upgrade*. European Centre for Medium Range Weather Forecasts Reading, UK.

Heming, J. T., Prates, F., Bender, M. A., Bowyer, R., Cangialosi, J., Caroff, P., … others (2019). Review of recent progress in tropical cyclone track forecasting and expression of uncertainties. *Tropical Cyclone Research and Review*, *8*(4), 181–218.

Hermes, J. C., & Reason, C. J. (2009). The sensitivity of the seychelles–chagos thermocline ridge to large-scale wind anomalies. *ICES Journal of Marine Science*, *66*(7), 1455–1466.

Hoarau, G., & Malardel, S. (2021). *Oceanic evaluation of the AROME-NEMO coupled system by ALAMO float measurements: Case of cyclone FLORENCE.* Retrieved from https://www.umr-cnrm.fr/IMG/pdf/r_r_2021-en_web.pdf

Hoarau, T., Barthe, C., Tulet, P., Claeys, M., Pinty, J.-P., Bousquet, O., ... Vié, B. (2018). Impact of the generation and activation of sea salt aerosols on the evolution of tropical cyclone dumile. *Journal of Geophysical Research: Atmospheres: Atmospheres*, *123*(16), 8813– 8831.

Houze, R. A. (2010). Clouds in tropical cyclones. *Monthly Weather Review*, *138*, 293-344.

Jullien, S., Marchesiello, P., Menkes, C. E., Lefèvre, J., Jourdain, N. C., Samson, G., & Lengaigne, M. (2014). Ocean feedback to tropical cyclones: Climatology and processes. *Climate dynamics*, *43*(9-10), 2831–2854.

Jullien, S., Menkès, C. E., Marchesiello, P., Jourdain, N. C., Lengaigne, M., Koch-Larrouy, A., ... Faure, V. (2012). Impact of tropical cyclones on the heat budget of the south pacific ocean. *Journal of Physical Oceanography*, *42*(11), 1882–1906.

Kossin, J. P., McNoldy, B. D., & Schubert, W. H. (2002). Vortical swirls in hurricane eye clouds. *Monthly Weather Review*, *130*(12), 3144 - 3149. doi: 10.1175/1520-0493(2002)130⟨3144:VSIHEC⟩2.0.CO;2

Lebeaupin Brossier, C., Ducrocq, V., & Giordani, H. (2009). Two-way one-dimensional high-resolution air–sea coupled modelling applied to mediterranean heavy rain events. *Quarterly Journal of the Royal Meteorological Society: A journal of the atmospheric sciences, applied meteorology and physical oceanography*, *135*(638), 187–204.

Lellouche, J.-M., Greiner, E., Le Galloudec, O., Garric, G., Regnier, C., Drevillon, M., ... others (2018). Recent updates to the copernicus marine service global ocean monitoring and forecasting real-time 1/ 12° high-resolution system. *Ocean Science*, *14*(5), 1093–1126.

Leroux, M.-D., Meister, J., Mekies, D., Dorla, A.-L., & Caroff, P. (2018). A climatology of southwest indian ocean tropical systems: Their number, tracks, impacts, sizes, empirical maximum potential intensity, and intensity changes. *Journal of Applied Meteorology and Climatology*, *57*(4), 1021–1041.

Lin, I., Wu, C.-C., Pun, I.-F., & Ko, D.-S. (2008). Upper-ocean thermal structure and the western north pacific category 5 typhoons. part i: Ocean features and the category 5 typhoons' intensification. *Monthly Weather Review*, *136*(9), 3288–3306.

Madec, G., Bourdallé-Badie, R., Chanut, J., Clementi, E., Coward, A., Ethé, C., ... Samson, G. (2019, October). *Nemo ocean engine.* Zenodo. Retrieved from `https://doi.org/10.5281/zenodo.3878122` (Add SI3 and TOP reference manuals) doi: 10.5281/zenodo.3878122

Madec, G., Delecluse, P., Imbard, M., & Lévy, C. (1998). Opa 8.1 ocean general circulation model reference manual. *Note du Pôle de modélisation*, *11*, 91p.

Madec, G., & Imbard, M. (1996). A global ocean mesh to overcome the north pole singularity. *Climate Dynamics*, *12*(6), 381–388.

Magnusson, L., Bidlot, J.-R., Bonavita, M., Brown, A., Browne, P., De Chiara, G., ... others (2019). Ecmwf activities for improved hurricane forecasts. *Bulletin of the American Meteorological Society*, *100*(3), 445–458.

Mogensen, K. S., Magnusson, L., & Bidlot, J.-R. (2017). Tropical cyclone sensitivity to ocean coupling in the e cmwf coupled model. *Journal of Geophysical Research: Oceans*, *122*(5), 4392–4412.

Mouche, A. A., Chapron, B., Zhang, B., & Husson, R. (2017). Combined co-and cross-polarized sar measurements under extreme wind conditions. *IEEE Transactions on Geoscience and Remote Sensing*, *55*(12), 6746–6755.

Pianezze, J., Barthe, C., Bielli, S., Tulet, P., Jullien, S., Cambon, G., ... Cordier, E. (2018). A new coupled ocean-waves-atmosphere model designed for tropical storm studies: example of tropical cyclone bejisa (2013–2014) in the south-west indian ocean. *Journal of Advances in Modeling Earth Systems*, *10*(3), 801–825.

Pineau-Guillou, L., Ardhuin, F., Bouin, M.-N., Redelsperger, J.-L., Chapron, B., Bidlot, J.-R., & Quilfen, Y. (2018). Strong winds in a coupled wave–atmosphere model during a north atlantic storm event: Evaluation against observations. *Quarterly Journal of the Royal Meteorological Society*, *144*(711), 317–332.

Price, J. F. (1981). Upper ocean response to a hurricane. *Journal of Physical Oceanography*, *11*(2), 153–175.

Sauvage, C., Lebeaupin Brossier, C., Bouin, M.-N., & Ducrocq, V. (2020).

Characterization of the air–sea exchange mechanisms during a mediterranean heavy precipitation event using realistic sea state modelling. *Atmospheric Chemistry and Physics*, *20*(3), 1675–1699. Retrieved from `https://acp.copernicus.org/articles/20/1675/2020/` doi: 10.5194/acp-20-1675-2020

Schade, L. R., & Emanuel, K. A. (1999). The ocean's effect on the intensity of tropical cyclones: Results from a simple coupled atmosphere–ocean model. *Journal of the Atmospheric Sciences*, *56*(4), 642–651.

Seity, Y., Brousseau, P., Malardel, S., Hello, G., Bénard, P., Bouttier, F., ... Masson, V. (2011). The arome-france convective-scale operational model. *Monthly Weather Review*, *139*(3), 976–991.

Srinivas, C., Mohan, G. M., Naidu, C., Baskaran, R., & Venkatraman, B. (2016). Impact of air-sea coupling on the simulation of tropical cyclones in the north indian ocean using a simple 3-d ocean model coupled to arw. *Journal of Geophysical Research: Atmospheres*, *121*(16), 9400–9421.

Vellinga, M., Copsey, D., Graham, T., Milton, S., & Johns, T. (2020). Evaluating benefits of two-way ocean–atmosphere coupling for global nwp forecasts. *Weather and Forecasting*, *35*(5), 2127–2144.

Vialard, J., Foltz, G., Mcphaden, M. J., Duvel, J.-P., & de Boyer Montégut, C. (2008). Strong indian ocean sea surface temperature signals associated with the madden-julian oscillation in late 2007 and early 2008. *Geophysical Research Letters*, *35*(19).

Vincent, E. M., Lengaigne, M., Madec, G., Vialard, J., Samson, G., Jourdain, N., ... Jullien, S. (2012b). Processes setting the characteristics of sea surface cooling induced by tropical cyclones. *Journal of Geophysical Research: Oceans*, *117*(C2).

Vincent, E. M., Lengaigne, M., Vialard, J., Madec, G., Jourdain, N., & Masson, S. (2012a). Assessing the oceanic control on the amplitude of sea surface cooling induced by tropical cyclones. *Journal of Geophysical Research: Oceans*, *117*(C5).

Voldoire, A., Decharme, B., Pianezze, J., Lebeaupin Brossier, C., Sevault, F., Seyfried, L., ... others (2017). Surfex v8. 0 interface with oasis3-mct to couple atmosphere with hydrology, ocean, waves and sea-ice models, from coastal to global scales. *Geoscientific Model Development*, *10*(11), 4207–4227.

Weill, A., Eymard, L., Caniaux, G., Hauser, D., Planton, S., Dupuis, H., ... others (2003). Toward a better determination of turbulent air–sea fluxes from several experiments. *Journal of Climate*, *16*(4), 600–618.

Yablonsky, R. M. (2016). Ocean component of the hwrf coupled model and model evaluation. In *Advanced numerical modeling and data assimilation techniques for tropical cyclone prediction* (pp. 267–304). Springer.

Yablonsky, R. M., & Ginis, I. (2009). Limitation of one-dimensional ocean models for coupled hurricane–ocean model forecasts. *Monthly Weather Review*, *137*(12), 4410–4419.